Environment as a limiting factor of the historical global spread of mungbean

Pei-Wen Ong[1], Ya-Ping Lin[2,3], Hung-Wei Chen[2], Cheng-Yu Lo[2], Marina Burlyaeva[4], Thomas Noble[5], Ramakrishnan Nair[6], Roland Schafleitner[3], Margarita Vishnyakova[4], Eric Bishop-von-Wettberg[7,8], Maria Samsonova[8], Sergey Nuzhdin[9], Chau-Ti Ting[10], Cheng-Ruei Lee[1,2]*

1. Institute of Plant Biology, National Taiwan University, Taipei 10617, Taiwan

2. Institute of Ecology and Evolutionary Biology, National Taiwan University, Taipei 10617, Taiwan

3. World Vegetable Center Headquarter, Tainan 74199, Taiwan

4. Federal Research Centre All-Russian N.I. Vavilov Institute of Plant Genetic Resources (VIR), St. Petersburg, Russia

5. Australian Department of Agriculture and Fisheries, Warwick, Queensland 4370, Australia

6. World Vegetable Center South and Central Asia, ICRISAT Campus, Patancheru, Hyderabad, Telangana 502324, India

7. Department of Plant and Soil Science and Gund Institute for the Environment, University of Vermont, Burlington, VT 05405, USA

8. Department of Applied Mathematics, Peter the Great St. Petersburg Polytechnic University, St. Petersburg, Russia

9. University of Southern California, Los Angeles, CA 90089, USA

10. Department of Life Science, National Taiwan University, Taipei 10617, Taiwan

* Author of correspondence

Cheng-Ruei Lee

chengrueilee@ntu.edu.tw

Abstract

While the domestication history has been investigated in many crops, the process of cultivation range expansion and factors governing this process received relatively little attention. Here using mungbean (*Vigna radiata* var. *radiata*) as a test case, we investigated the genomes of more than one thousand accessions to illustrate climatic adaptation's role in dictating the unique routes of cultivation range expansion. Despite the geographical proximity between South and Central Asia, genetic evidence suggests mungbean cultivation first spread from South Asia to Southeast, East, and finally reached Central Asia. Combining evidence from demographic inference, climatic niche modeling, plant morphology, and records from ancient Chinese sources, we showed that the specific route was shaped by the unique combinations of climatic constraints and farmer practices across Asia, which imposed divergent selection favoring higher yield in the south but short-season and more drought-tolerant accessions in the north. Our results suggest that mungbean did not radiate from the domestication center as expected purely under human activity, but instead the spread of mungbean cultivation is highly constrained by climatic adaptation, echoing the idea that human commensals are more difficult to spread through the south-north axis of continents.

Main Text

Introduction

Domestication is a process where plants or animals were cultivated by humans, leading to associated genetic and morphological changes. These changes may be intentional from human selection or unintentional as a result of adaptation to the environments of cultivation (Fuller, 2007). Later, the cultivated plants spread out from their initial geographical range (Meyer and Purugganan, 2013), and elucidating the factors affecting the range expansion of crops is another focus of active research (Gutaker et al., 2020). In the old world, during the process of "prehistory food globalization" (Jones et al., 2011), crops originated from distinct regions were transported and grown in Eurasia. Archeological evidence has shown that such "trans-Eurasian exchange" had happened by 1500 BC (Liu et al., 2019), and the proposed spread routes from archeological studies were supported by modern genetic evidence especially in rice (Gutaker et al., 2020) and barley (Lister et al., 2018). Interestingly, the spread may accompany genetic changes for the adaptation to novel environments. For example, in barley, variations in the gene *Photoperiod-H1* (*Ppd-H1*) resulting in the non-responsiveness to longer daylengths were likely associated with the historical expansion to high-latitude regions (Jones et al., 2008; Jones et al., 2016). While these mid-latitude cereals have been extensively studied, investigations of crops originated from other climate zones are needed. Using the South Asian legume mungbean as a test case, here we investigate how climatic adaptation might affect crop spread route and the evolutionary changes making such spread possible.

Mungbean (*Vigna radiata* (L.) Wilczek var. *radiata*), also known as green gram, is an important grain legume in Asia (Nair and Schreinemachers, 2020), providing carbohydrates, protein, folate, and iron for local diets and thereby contributing to food security (Kim et al., 2015). Among pulses, mungbean is capable of tolerating moderate drought or heat stress and has a significant role in rainfed agriculture across arid and semi-arid areas (Pratap et al., 2019), which are likely to have increased vulnerabilities to climate change. Although there have been studies about the genetic diversity of cultivated and wild mungbean (Ha et al., 2021; Kang et al., 2014; Noble et al., 2018; Sangiri et al., 2007), the evolutionary history of cultivated mungbean after domestication still lacks genetic studies. Existing archeological evidence suggests that South Asia

is the probable area of mungbean domestication, and at least two independent domestication events have been suggested, including Maharashtra and the eastern Harappan zone (Fuller and Harvey, 2006). The early archeological records suggest that the selection of large seed sizes occurred in the eastern Harappan zone by the 3rd millennium BC and in Maharashtra, dating to the late 2nd to early 1st millennium BC (Fuller and Harvey, 2006). This pulse later spread to mainland Southeast Asia and has been reported in southern Thailand dating to the late first millennium BC (Castillo et al., 2016). Further north, the earliest record of mungbean in China was from the book Qimin Yaoshu (齊民要術, 544 AD). While mungbean is also cultivated in Central Asia today, it was not identified in archaeobotanical evidence ranging from several millennium BC to the medieval period (Miller, 1999; Spengler et al., 2018b; Spengler et al., 2017), suggesting later arrival. While the archaeobotanical studies elucidated the route of mungbean cultivation range expansion, researches are still needed to identify the genetic evidence and factors shaping such spread route.

A recent genetic study revealed that present-day cultivated mungbeans have the same haplotype in the promoter region reducing the expression of *VrMYB26a* (Lin et al., 2022), a candidate gene controlling the important domestication trait, pod shattering, in several *Vigna* species (Takahashi et al., 2020). This suggests the loss of pod shattering phenotype in cultivated mungbean may have a common origin, and despite the archaeobotanical findings of several independent early cultivations of mungbean in South Asia (Fuller and Harvey, 2006), descendants from one of these cultivation origins might have dominated South Asia before the pan-Asia expansion. Since large regions remain archaeologically unexplored, utilization of genetic data can be a crucial complementation to reconstruct crop evolutionary history. Using seed proteins (Tomooka et al., 1992) and isozymes (Dela Vina and Tomooka, 1994), previous studies proposed two expansion routes out of India, one in the south to Southeast Asia and the other in the north along the silk road to China. While later studies used DNA markers to investigate mungbean population structure (Breria et al., 2020; Gwag et al., 2010; Islam and Blair, 2018; Noble et al., 2018; Sandhu and Singh, 2021; Sangiri et al., 2007), few have examined these hypothesized routes in detail. Therefore, genomic examination of the cultivation rage expansion proposed by archaeobotanical studies and the elucidation of its contributing factors are strongly needed.

In this study, we compiled an international effort, reporting a global mungbean diversity panel of more than 1,100 accessions derived from (i) the mungbean mini-core collection of the World Vegetable Centre (WorldVeg) genebank, (ii) the Australian Diversity Panel (ADP), and (iii) the Vavilov Institute (VIR), which hosts a one-century-old collection enriched with mid-latitude Asian accessions that are underrepresented in other genebanks, many of which were old landraces collected by Nikolai I. Vavilov and his teams in the early 20th century (Burlyaeva et al., 2019). These germplasms harbor a wide range of morphological variations (Figure 1A) and constitute the most comprehensive representation of worldwide mungbean genetic variation. We used this resource to investigate the global history of mungbean after domestication to reveal a spread route highly affected by climatic constraints across Asia, eventually shaping the phenotypic characteristics for local adaptation to distinct environments.

Results

Population structure and spread of mungbean

Using DArTseq, we successfully obtained new genotype data of 290 mungbean accessions from VIR (Supplementary file 1). Together with previous data (Breria et al., 2020; Noble et al., 2018), our final set included 1,108 samples with 16 wild and 1,092 cultivated mungbean. A total of 40,897 single nucleotide polymorphisms (SNPs) were obtained. Of these, 34,469 bi-allelic SNPs, with a missing rate less than 10%, were mapped on 11 chromosomes and retained for subsequent analyses.

The genetic structure was investigated based on the 10,359 LD-pruned SNPs. Principal component analysis (PCA, Figure 1C) showed a triangular pattern of genetic variation among cultivated mungbeans, consistent with previous studies (Breria et al., 2020; Noble et al., 2018; Sokolkova et al., 2020) and ADMIXTURE K = 3 (Figure 1B). The geographic distribution of these genetic groups is not random, as these three groups are distributed in South Asia (India and Pakistan), Southeast Asia (Cambodia, Indonesia, Philippines, Thailand, Vietnam, and Taiwan), and more northernly parts of Asia (China, Korea, Japan, Russia, and Central Asia). As K increased, the cross-validation (CV) error decreased a little after K = 4 (Figure 1-figure supplement 1), where the north group could be further divided (Figure 1B). Therefore, worldwide diversity of cultivated mungbean could be separated into four major genetic groups corresponding

129 to their geography: South Asian (SA), Southeast Asian (SEA), East Asian (EA), and Central
130 Asian (CA) groups. Note that the genetic groups were named after the region where most of their
131 members distribute, and exceptions exist. For example, many EA accessions also distribute in
132 Central Asia, and some SEA accessions were found near the eastern and northeastern coasts of
133 India. Throughout this work, we make clear distinction between genetic group names (e.g., SA)
134 and a geographic region (e.g., South Asia). Therefore, unlike any other previous work in this
135 species, this study incorporates global genetic variation among cultivated mungbean of this
136 important crop.

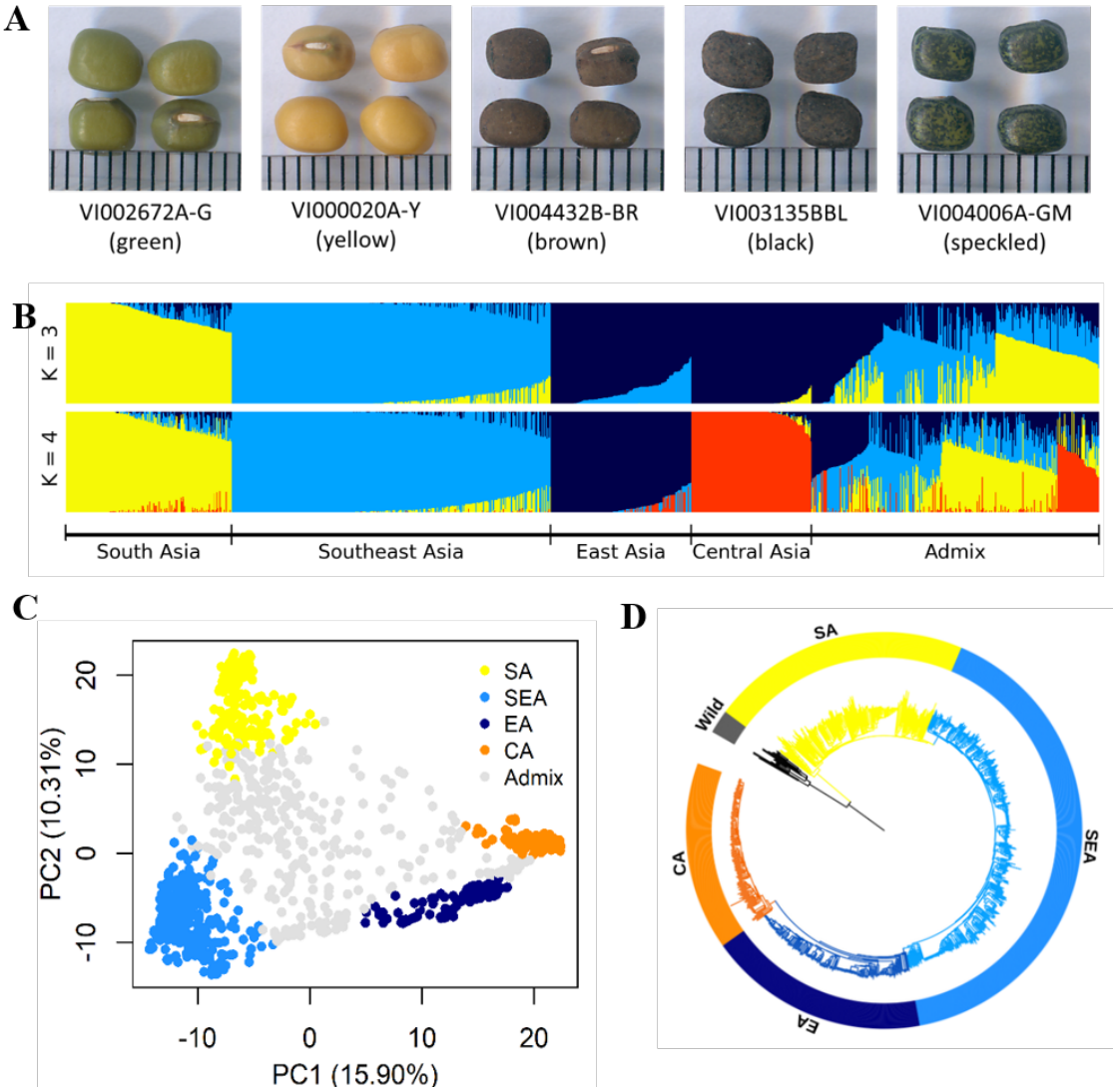

Figure 1. Diversity of worldwide mungbean. (A) Variation in seed colour. (B) ADMIXTURE ancestry coefficients, where accessions were grouped by group assignments ($Q \geq 0.7$). (C) Principal component analysis (PCA) plot of 1,092 cultivated mungbean accessions. Accessions were coloured based on their assignment to four inferred genetic groups ($Q \geq 0.7$), while accessions with $Q < 0.7$ were coloured gray. (D) Neighbor-joining (NJ) phylogenetic tree of 788 accessions with $Q \geq 0.7$ with wild mungbean as outgroup (black colour).

Using wild progenitor *V. radiata* var. *sublobata* (Wild hereafter) as the outgroup, the accession-level (Figure 1D) and population-level (Figure 2A) phylogenies both suggest CA to be genetically closest to EA. The SEA group is more distant, and SA is the most diverged. This relationship is supported by the outgroup *f*3 tests showing EA and CA share the most genetic drift, followed by SEA and SA (Supplementary file 2). Pairwise F_{ST} and d_{xy} also give the same conclusion (Figure 2B). Similarly, the *f*4 tests (Figure 2C) strongly reject the cases where SEA and CA form a clade relative to SA and EA (*f*4(SA,EA;SEA,CA) = 0.016, $Z = 9.519$) or SEA and EA form a clade relative to SA and CA (*f*4(SA,CA;SEA,EA) = 0.021, $Z = 13.956$), again suggesting EA and CA to be closest. With regards to the relationship among Wild, SA, SEA, and EA, *f*4 tests suggest SEA and EA form a clade relative to Wild and SA (non-significant results in *f*4(Wild,SA;EA,SEA) but opposite in other combinations). Notably, both TreeMix (Figure 2A) and the *f*4 test (Figure 2C, *f*4(SA,SEA;CA,EA) = 0.005, $Z = 6.843$) suggest gene flow between SEA and EA. Consistent with archeological evidence of South Asian domestication, the nucleotide diversity (π) decreased from SA (1.0×10^{-3}) to SEA (7.0×10^{-4}) and EA (5.0×10^{-4}), while the CA group has lowest diversity (3.0×10^{-4}) (Figure 2B). LD also decays the fastest in Wild and then the SA group (Figure 2D), followed by other genetic groups. In summary, all analyses are consistent with our proposed order of cultivated mungbean divergence.

Our proposed demographic history could be confounded by factors such as complex hybridization among groups. For example, SEA and CA might have independently originated from SA and later generated a hybrid population in EA (Figure 2-figure supplement 1A). Other possibilities are that either SEA or CA are the hybrid of other populations (Figure 2-figure supplement 1B and C). We examined these possibilities using *f*3 statistics for all possible trios among the four groups. None of the tests gave a significantly negative *f*3 value (Supplementary file 3), suggesting the lack of a strong alternative model to our proposed relationship among these four groups.

Based on the solid relationship among these genetic groups, we used fastsimcoal2 to model their divergence time, allowing population size change and gene flow at all time points (Figure 2-figure supplement 2A-D). According to this model, after initial domestication, the out-of-India event (when other groups diverged from SA) happened about 8.3 thousand generations ago (kga) with 75% parametric bootstrap range between 4.7 and 11.3 kga. Not until more than

five thousand generations later (2.7 kga, 75% range 1.1-4.6 kga) did SEA diverge from the common ancestor of present-day EA and CA. CA diverged from EA only very recently (0.2 kga, 75% range 0.1-0.8 kga). Note that the divergence time was estimated in the number of generations, and the much longer growing seasons in the southern parts of Asia may allow more than one cropping season per year (Mishra et al., 2022; Vir et al., 2016).

Our results suggest the non-South-Asian accessions have a common origin out of India (otherwise these groups would branch off independently from the SA group). Given this, the phylogenetic relationship (Figure 2A) is consistent with the following hypotheses. (1) The east hypothesis: Mungbean expanded eastwards and gave rise to the SEA group. This group might initially occupy northeast South Asia and later expanded to Southeast Asia either through the land or maritime route (Castillo et al., 2016; Fuller et al., 2011). The group later expanded northwards as EA. EA expanded westwards into Central Asia and gave rise to the CA group. (2) The north hypothesis: The group leaving South Asia first entered Central Asia as the EA group. EA expanded eastwards into East Asia through the Inner Asian Mountain Corridor (Stevens et al., 2016). The eastern population of EA expanded southwards as the SEA group, and later the western population of EA diverged as the CA group. (3) The northeast hypothesis: The group leaving South Asia (through either of the above-mentioned routes) was first successfully cultivated in northern East Asia without previously being established in Southeast Asia or Central Asia. The EA group then diverged southwards as SEA and later expanded westwards, giving rise to CA. Consistent with this model, the genetic variation of the EA group gradually declines from east to west, accompanied by the gentlest decline of precipitation per unit geographic distance across Asia (Figure 2F).

While all three hypotheses are consistent with the phylogeny (Figure 2A), the SEA group originated earlier than EA in the east hypothesis but later in the two other hypotheses. The former case predicts higher nucleotide diversity and faster linkage disequilibrium decay in SEA than EA, which is supported by our results (Figure 2B and D). While populations that were established in a region for an extended time could accumulate genetic differentiation, generating patterns of isolation by distance, rapid-spreading populations in newly colonized regions could not (Lee et al., 2017; The 1001 Genomes Consortium, 2016). Using this idea, Mantel's test revealed a significantly positive correlation between genetic and geographic distances for the SA genetic

group ($r = 0.466$, $P = 0.010$), followed by SEA ($r = 0.252$, although not as significant, $P = 0.069$). No such association was found for EA ($r = 0.030$, $P = 0.142$) or CA ($r = 0.087$, $P = 0.172$). In addition, the southern groups (SA and SEA) together ($r = 0.737$, $P = 0.001$) have a much stronger pattern of isolation by distance than the northern groups (EA and CA, $r = 0.311$, $P = 0.001$) (Figure 2E). Using $Q \geq 0.5$ instead of $Q \geq 0.7$ to assign individuals into genetic groups generated results that are largely consistent (Supplementary file 4). These results are again consistent with the "east hypothesis" that local accessions from the SA and SEA groups were established much earlier than those from EA and CA. Finally, the genetic variation of the EA group is highest in the eastern end and declines westwards (Figure 2F). This does not support the north hypothesis where EA first existed in Central Asia and expanded eastwards.

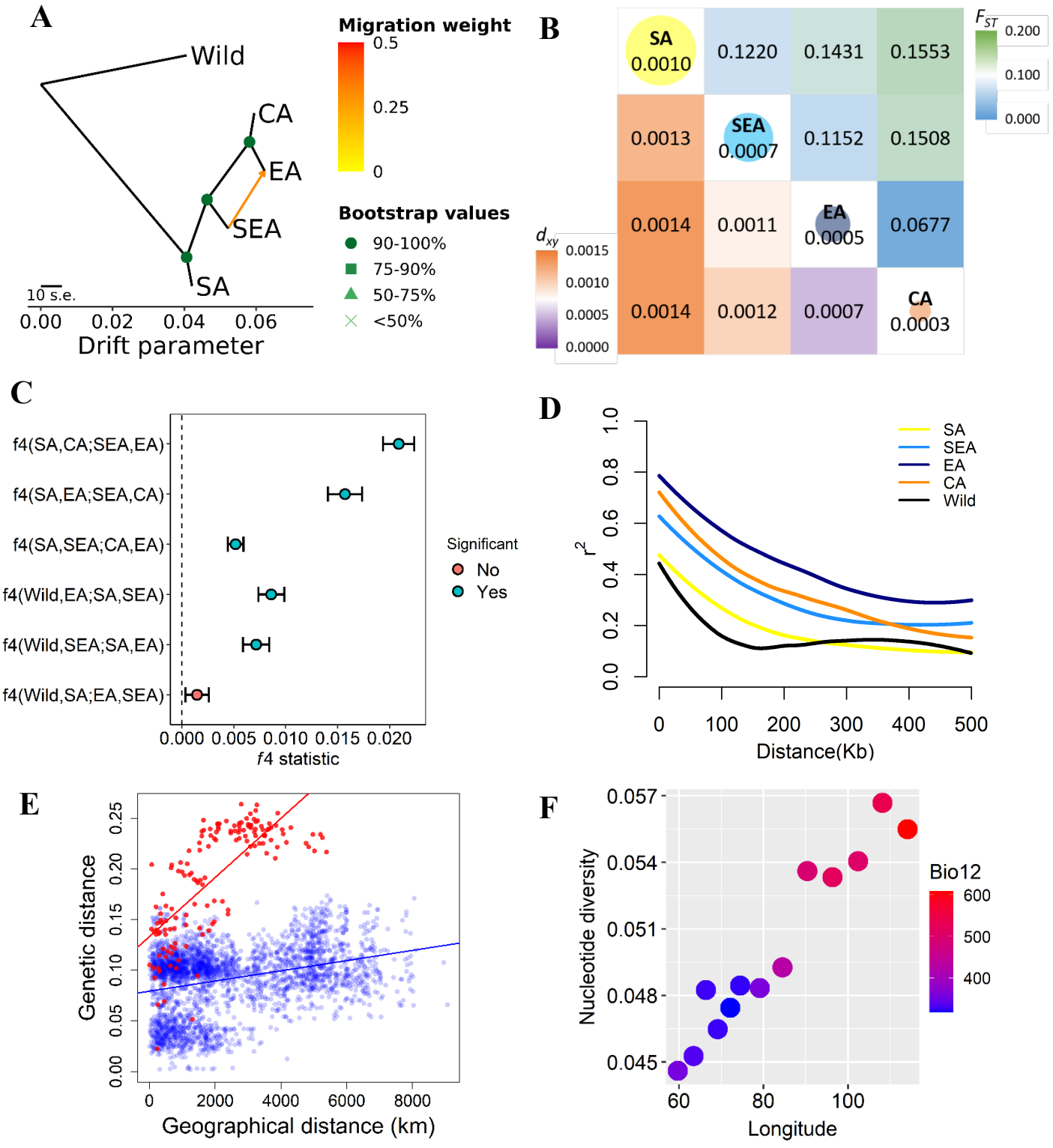

Figure 2. Fine-scale genetic relationship and admixture among four inferred genetic groups. (A) TreeMix topologies with one suggested migration event. Colours on nodes represent support values after 500 bootstraps. (B) Diversity patterns within and between inferred genetic groups as estimated using nucleotide diversity (π in diagonal, where the size of the circle represents the level of π) and population differentiation (F_{ST} in upper diagonal and d_{xy} in lower diagonal). (C) f_4 statistics. Points represent the mean f_4 statistic and lines are the standard error. Only f_4 statistics with Z-score > |3| are considered statistically significant. The dashed line denotes $f_4 = 0$. (D) Linkage disequilibrium (LD) decay. (E) Isolation by distance plot of genetic distance versus geographic distance, with the southern group in red circles and the northern group in blue circles. (F) Relationship between Bio12 (annual precipitation) and nucleotide diversity (π) of the EA genetic group across the east-west axis of Asia. Dot colors represent the annual precipitation of each population.

209

Environmental differentiation of the inferred genetic groups

We further examined the possible causes governing the expansion of mungbean cultivation ranges. For a crop to be successfully cultivated in a new environment, dispersal and adaptation are both needed. Being a crop that has lost the ability of pod shattering, the spread of mungbean was governed by commerce or seed exchange. While barriers such as the Himalayas or Hindu Kush may limit human activity, South and Central Asia was already connected by a complex exchange network linking the north of Hindu Kush, Iran, and the Indus Valley as early as about 4 thousand years ago (kya) (Dupuy, 2016; Kohl, 2007; Kohl and Lyonnet, 2008; Lamberg-Karlovsky, 2002; Lombard, 2020; Lyonnet, 2005), and some sites contain diverse crops originated across Asia (Spengler et al., 2021). Similarly, other ancient land or maritime exchange routes existed among South, Southeast, East, and Central Asia (Stevens et al., 2016). This suggests that mungbean could have been transported from South to Central Asia, but our genetic evidence suggests that the present-day CA group did not descend directly from the SA group. Therefore, we investigated whether climatic adaptation, that is, the inability of mungbean to establish in a geographic region after human-mediated long-range expansion, could be a contributing factor.

Multivariate analysis of variance (MANOVA) of eight bioclimatic variables (after removing highly-correlated ones; Supplementary file 5 and 6) indicated strong differentiation in the environmental niche space of the four genetic groups (Supplementary file 7 and 8). PCA of climatic factors clearly reflects geographic structure, where the axis explaining most variation (PC1, 42%) separates north and south groups and is associated with both temperature- and precipitation-related factors (Figure 3A and Supplementary file 9). Consistent with their geographic distribution, overlaps between EA and CA and between SA and SEA were observed. While these analyses were performed using bioclimatic variables from year-round data, we recognized that summer is the cropping season in the north. Parallel analyses using the temperature and precipitation of May, July, and September yielded similar results (Supplementary file 10; Figure 3-figure supplement 1).

Based on the Köppen climate classification (Köppen, 2011), we categorized the Asian mungbean cultivation range into six major climate zones (Figure 3-figure supplement 2): dry hot (BSh and BWh), dry cold (BSk and BWk), temperate dry summer (Csa), tropical savanna (Aw),

Continental (Dwb and Dfb), and temperate wet summer (Cfa and Cwa). The former three are relatively drier than the latter three zones. While SEA and CA are relatively homogeneous, SA and EA have about half of the samples in the dry and non-dry zones (Figure 3-figure supplement 2). We therefore separated SA into SAe and SAw and EA into EAe and EAw, corresponding to the wetter eastern and drier western regions within the SA and EA ranges. Environmental niche modeling revealed distinct suitable regions of these six groups except for CA and EAw, whose geographical ranges largely overlap (Figure 3B). Consistent with PCA, pairwise Schoener's D values are smallest between the northern and southern groups while largest (suggesting overlaps of niche space) between the eastern and western subsets within north and south (Figure 3B), consistent with PCA that the major axis of climatic difference is between the northern and southern parts of Asia. Analyses using temperature and precipitation from May, July, and September yielded similar results (Figure 3-figure supplement 3). Given a single out-of-India event (Figure 2A), the results suggest it might be easier to first cultivate mungbean in Southeast rather than Central Asia, supporting the east hypothesis.

While both temperature and precipitation variables differ strongly between north and south, one should note that these year-round temperature variables do not correctly reflect conditions in the growing seasons. In the north, mungbean is mostly grown in summer where the temperature is close to the south (Figure 3-figure supplement 4A-C). On the other hand, precipitation differs drastically between the north and south, especially for the CA group, where the summer growing season is the driest of the year (Figure 3-figure supplement 4D). By estimating the regression slope of annual precipitation on geographical distance, we obtained a gradient of precipitation change per unit geographic distance between pairs of genetic groups (Figure 3C). Despite the SA-SEA transect having the steepest gradient (slope = 0.21), the spread from SA to SEA has been accompanied by an increase of precipitation and did not impose drought stress. However, the second highest slope (0.18) is associated with a strong precipitation decrease if the SA group were to disperse to Central Asia. Results from the precipitation of May, July, and September yielded similar conclusion (Figure 3-figure supplement 5). This likely explains why no direct historic spread is observed from South to Central Asia.

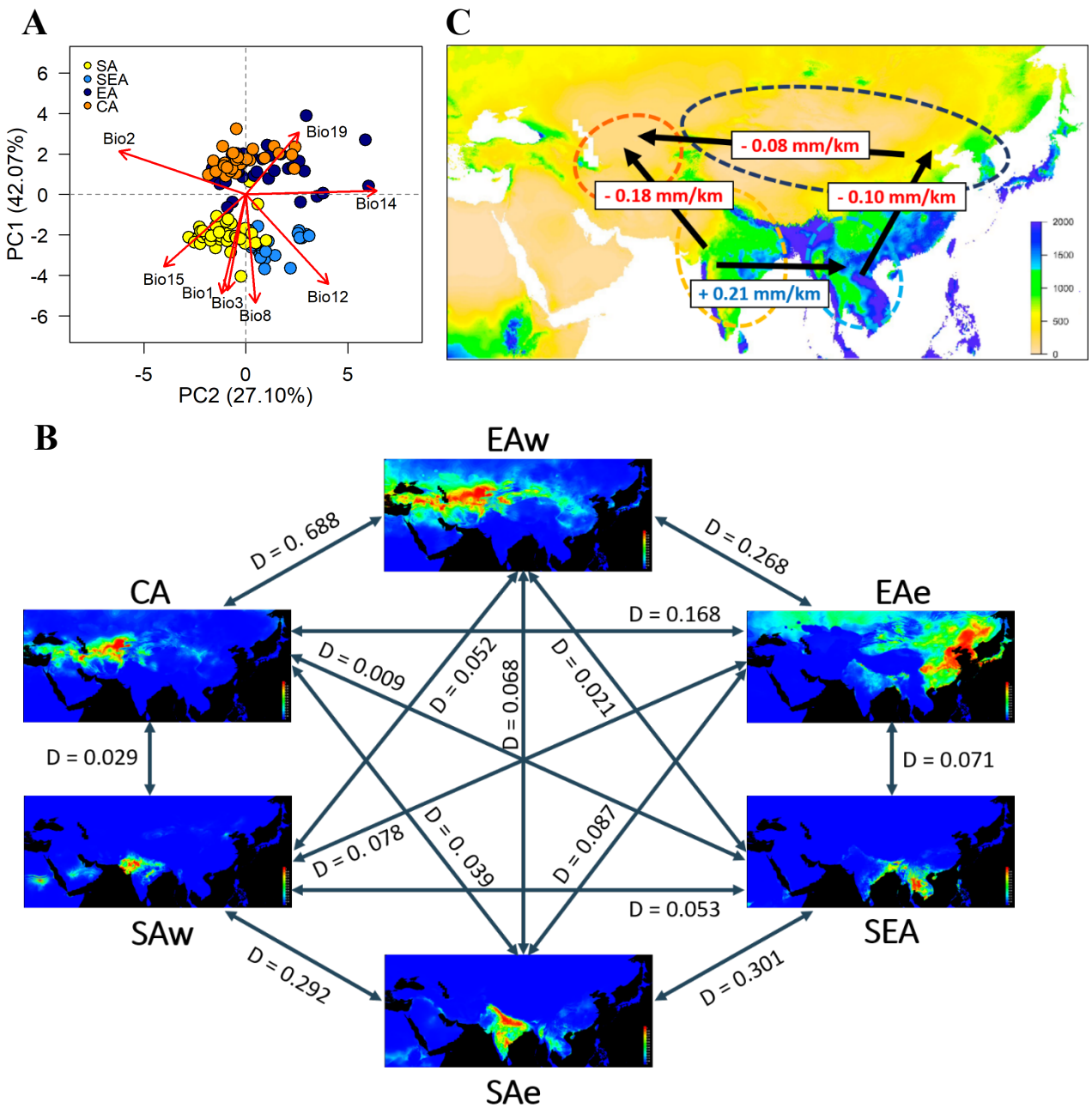

Figure 3. Environmental variation among genetic groups of mungbean. (A) Principal component analysis (PCA) of the eight bioclimatic variables. Samples are coloured according to four inferred genetic groups as indicated in the legend. (B) Predicted distribution at current climate conditions. Red colour indicates high suitability, and blue indicates low suitability. Values between pairs represent niche overlap measured using Schoener's D, and higher values represent higher overlaps. Abbreviations: SAw: South Asia (west), SAe: South Asia (east); SEA: Southeast Asia; EAe: East Asia (east); EAw: East Asia (west) and CA: Central Asia. (C) Environmental gradient across potential directions of expansion. The value on each arrow indicates a change in annual precipitation per kilometer. The background map is colored according to annual precipitation (Bio12, in mm).

Trait variation among genetic groups

If environmental differences constrained the spread route of mungbean, the current cultivated mungbean accessions occupying distinct environments should have locally adaptive traits for these environments. Indeed, PCA of four trait categories show substantial differences among genetic groups (phenology, reproductive output, and size in field trials, as well as plant weight in lab hydroponic systems, Figure 4A). In the field, CA appears to have the shortest time to flowering, the lowest yield in terms of seed size and pod number, and the smallest leaf size (Figure 4B and Supplementary file 11). On the other hand, SEA accessions maximize seed size, while SA accessions specialize in developing the largest number of pods (Figure 4B). These results suggest that CA has a shorter crop duration, smaller plant size, and less yield, consistent with drought escape phenotypes. This is consistent with the northern short growing season constrained by temperature and daylength (below), as well as the low precipitation during the short season.

In terms of seedling response to drought stress, the Q_{ST} values of most traits (root, shoot, and whole plant dry weights under control and drought treatments) are higher than the tails of SNP F_{ST}, suggesting trait evolution driven by divergent selection (Figure 4C; Figure 4-figure supplement 6). Significant treatment, genetic group, and treatment by group interaction effects were observed except on a few occasions (Table 1). Consistent with field observation, SEA has the largest seedling dry weight (Figure 4D). While simulated drought significantly reduced shoot dry weight for all groups, the effect on SEA is especially pronounced (treatment-by-group interaction effect, $F_{2,575} = 23.55$ $P < 0.001$, Table 1 and Figure 4D), consistent with its native habitats with abundant water supply (Figure 3-figure supplement 4D and Supplementary file 12). All groups react to drought in the same way by increasing root:shoot ratio (Figure 4D), suggesting such plastic change may be a strategy to reduce transpiration. Despite the lack of treatment-by-group interaction ($F_{2,575} = 1.39$, $P > 0.05$), CA consistently exhibits a significantly higher root:shoot ratio, a phenotype that is potentially adaptive to its native environment of lower water supply (Figure 3-figure supplement 4D and Supplementary file 12).

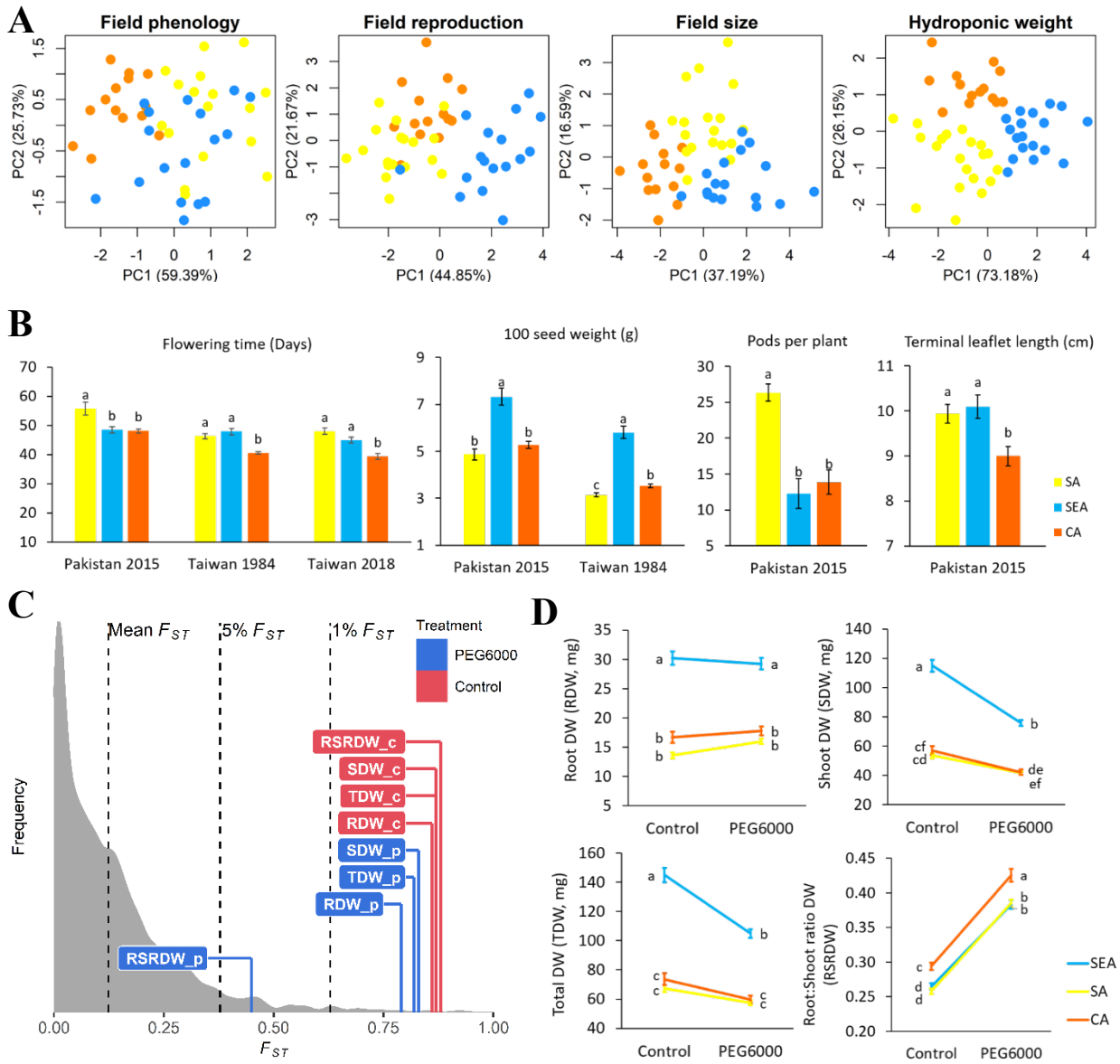

Figure 4. Quantitative trait differentiation among genetic groups. (A) Principal component analysis (PCA) of four trait categories. (B) Trait variability from common gardens in field experiments. (C) Comparison of Q_{ST}-F_{ST} for four drought-related traits under two environments. F_{ST} values (mean, 5% and 1%) were indicated by black dashed lines. The Q_{ST} for each trait was colored according to treatment and was calculated as Equation 2 in Materials and Methods. Abbreviations: RDW: root dry weight; SDW: shoot dry weight; TDW: total dry weight; RSRDW: root:shoot ratio dry weight; c: control; p: PEG6000. (D) Effect of PEG6000 (-0.6 MPa) on root dry weight (RDW), shoot dry weight (SDW), total dry weight (TDW), and root:shoot ratio dry weight (RSRDW) among genetic groups. Data were expressed as the mean ± standard error. Lowercase letters denote significant differences under Tukey's HSD in (B) and (D).

Table 1. Analysis of variance (ANOVA) *F* values for the dry weight (mg) of mungbean seedlings across three different genetic groups

Source of variation	df	RDW	SDW	TDW	RSRDW
Treatment	1	2.65$^{n.s.}$	133.26***	72.26***	978.76***
Genetic group	2	60.63***	79.62***	76.54***	13.27***
Treatment x Genetic group	2	3.29*	23.55***	17.79***	1.39$^{n.s.}$

(df: degrees of freedom; RDW: root dry weight; SDW: shoot dry weight; TDW: total dry weight; RSRDW: root:shoot ratio dry weight. Significance level * $P < 0.05$, *** $P < 0.001$, n.s. non-significant)

Support from ancient Chinese sources

Mungbean has been occasionally mentioned in ancient Chinese sources. Here we report the records associated with our proposed mungbean spread route and the underlying mechanisms. The "Classic of Poetry" (Shijing 詩經) contains poems dating between the 11th to 7th centuries BCE near the lower and middle reaches of the Yellow River. While crops (especially soy bean, 菽), vegetables, and many other plants have been mentioned, mungbean was not recorded. This is consistent with our results that mungbean had not reached the northern parts of East Asia at that time (the EA group diverged from the SEA group at around 2.7 kga). The first written record of mungbean in China is in an agricultural encyclopedia Qimin Yaoshu (齊民要術, 544 AD, Chinese text and translation in Supplementary note), whose spatiotemporal background (~1.5 kya near the lower reaches of Yellow River) is again consistent with our estimated origin of the EA group.

Our results suggest that the expansion of the mungbean cultivation range may be associated with the novel phenotypic characteristics potentially adaptive to the new environments. This proposal would be rejected if the novel phenotypic characteristics appeared very recently. In support of our proposal, Xiangshan Yelu (湘山野錄, an essay collection during 1068-1077 AD) recorded that mungbean from the southern parts of Asia had higher yield and larger grains than those in northern China (Chinese text and translation in Supplementary note). Similarly, Tiangong Kaiwu (天工開物, 1637 AD) mentioned that mungbean must be sown during July and August (Chinese text and translation in Supplementary note). The record suggests that the daylength requirement restricts the sowing period of mungbean in the north. Together with the

dry summer (Figure 3-figure supplement 4D) and soon-arriving autumn frost, there might be a strong selection favoring accessions with the rapid life cycle. These records suggest the phenotypic characteristics of northern accessions did not originate very recently, and the unique distribution of climatic zones in Asia resulted in not only the specific patterns of expansion but also the evolution of novel phenotypic characteristics in mungbean.

Discussion

Using mungbean as a test case, we combined population genomics, environmental niche modeling, empirical field and laboratory investigation, and ancient Chinese text analyses to demonstrate the importance of climatic adaptation in dictating the unique patterns of cultivation range expansion after domestication. In this study, we focus on how or when mungbean could be established as part of local agriculture throughout Asia. We showed that after leaving South Asia, mungbean was likely first cultivated in Southeast Asia, East Asia, and finally Central Asia. We acknowledge that our data do not allow us to specify the number of previous out-of-India events that did not leave traces in modern genetic data or their exact routes (for example, whether mungbean expanded from South to Southeast Asia through the land or maritime routes). While there might be multiple attempts to bring mungbean out of India as a commodity for consumption, our results suggest all present-day non-South-Asian accessions have a common out-of-India origin.

The climate-driven spread route despite historical human activities

Combining archeological records, population genetics, and niche modeling (Figure 2 and 3), our results suggest that after the early cultivation of mungbean in northwestern or southern South Asia (Fuller, 2007; Kingwell-Banham et al., 2015), the large environmental difference may restrict its northwards spread to Central Asia. Mungbean may first spread to eastern South Asia, and the subsequent expansion to Southeast Asia might be facilitated by the environmental similarity between these two regions. This is supported by archaeobotanical remains from the Thai-Malay Peninsula date to ca. 400-100 BCE (Castillo et al., 2016). It took more than five thousand generations until mungbean further spread to northeast Asia, again likely due to the environmental difference. The later appearance of mungbean in northern China is also supported by historical records. After that, the EA group spread across the northern part of Asia within a

few thousand generations. Our proposed route suggests that mungbean reached Central Asia at the latest, consistent with its absence from archeological sites in Central Asia, including Turkmenistan and Uzbekistan in the Chalcolithic and Bronze ages (5th to 2nd millennium BC) (Miller, 1999), Southeastern Kazakhstan in the Iron age dating 1st millennium BC (Spengler et al., 2017), and eastern Uzbekistan during the medieval period (800-1100 AD) (Spengler et al., 2018b). In addition, mungbean was only mentioned later by the 18th and early 19th centuries as a pulse grown in the Khiva region of Uzbekistan (Annanepesov and Bababekov, 2003).

In this study, we suggest that the ability to disperse may not be an essential factor restricting mungbean spread from South to Central Asia. Cultivated mungbean has lost the natural ability of pod shattering to disperse seeds, and they mostly traveled through landscapes by human-mediated seed exchange or commerce. Evidence of long-distance human-mediated dispersal of mungbean was available. For example, mungbean seeds have been found near the Red Sea coast of Egypt during the Roman (AD 1–250) period (Van der Veen and Morales, 2015). As early as about four kya, the Bactria–Margiana Archaeological Complex (BMAC) civilization north of the Hindu Kush had extensive contact with the Indus Valley Civilization (Dupuy, 2016; Kohl, 2007; Kohl and Lyonnet, 2008; Lamberg-Karlovsky, 2002; Lombard, 2020; Lyonnet, 2005). By 1,500 BC, the "Trans-Eurasian Exchanges" of major cereal crops has happened (Liu et al., 2019). The frequent crop exchange is evidenced by archaeobotanical findings in the Barikot site (ca. 1200 BC-50 AD) in northern Pakistan (Spengler et al., 2021), where diverse crops were cultivated, including those from West Asia (wheat, barley, pea, and lentil), South Asia (urdbean/mungbean), and likely East Asia (rice). Despite this, in Bronze-age archeological sites north of Hindu Kush, legumes (such as peas and lentils) were observed to a lesser extent than cereals, and South Asian crops were not commonly found (Jeong et al., 2019; Spengler, 2015; Spengler et al., 2014a; Spengler et al., 2018a; Spengler et al., 2014b). Interestingly, archeologists suggested legume's higher water requirement than cereals may be associated with this pattern, and pea and lentil's role as winter crops in Southwest Asia may be associated with their earlier appearance in northern Central Asia than other legumes (Spengler et al., 2014a; Spengler et al., 2018a; Spengler et al., 2014b). Therefore, despite the possibility of human-mediated seed dispersal between South and Central Asia, our results and archeological evidence concurred that mungbean arrived in Central Asia at the latest, likely restricted by environmental adaptation.

Local adaptation of mungbean genetic groups

Despite the profound impact of human-mediated dispersal on the spread of these and many other crops (Herniter et al., 2020; Kistler et al., 2018), in mungbean we suggest adaptation to distinct climatic regimes to be an important factor in the establishment after dispersal. Mungbean is commonly grown under rainfed cultivation and depends on the residual moisture in the fields after the primary crop, thus responding to water stress (Douglas et al., 2020). In the south, a temperature range of 20-30^{o}C and annual precipitation of 600-1,000 mm is optimal for mungbean (Ha and Lee, 2019). In Central Asia, however, the annual precipitation could be as low as 286 mm, greatly below the lower limit required for the southern mungbean. This situation could be further acerbated by the fact that mungbean might not be a highly valued crop under extensive care during cultivation. Indeed, the earliest record of mungbean in China (Qimin Yaoshu 齊民要術, 544 AD) emphasizes its use as green manure. In Central Asia, mungbean is a minor crop (Rani et al., 2018) grown with little input, only in the short duration between successive planting of main crops (which is also the dry season in Central Asia, Supplement file 12 and Figure 3-figure supplement 4) and using residual soil moisture with little irrigation. We suggest that the lack of extensive input subjects mungbean to more substantial local climatic challenges than highly valued high-input crops that receive intensive management, including irrigation. Therefore, the combination of climatic constraints and cultural usage, instead of physical barriers, may have shaped the historical spread route of the mungbean despite extensive human activities across the continent.

In addition to the constraint of soil moisture, other factors may have contributed to the selection of short-season accessions in the north. In the short summer seasons of much of Central Asia, short crop cycling is a requirement. In Uzbekistan, mungbean is often sown in early July after the winter wheat season and harvested before mid-October to avoid delays in the next round of winter wheat and escape frost damage. Therefore, fast-maturing accessions are essential for this production system (Rani et al., 2018). Similar rotation systems using mungbean to restore soil fertility during the short summer season after the harvest of the main crop were also mentioned in ancient Chinese sources (Chen, 1980). Mungbean is a short-day species from the south, and daylength likely limits the window when mungbean could be grown in the north:

Chinese texts during the 17th century (Tiangong Kaiwu 天工開物, 1637 AD) specifically mentioned the suitable duration to sow mungbean to control the flowering behavior for maximum yield (Supplementary note). Therefore, unlike in the south where yield appears to be an important selection target, the unique combination of daylength, agricultural practices, soil water availability, and frost damage in the north requires the selection for short-season accessions, likely limiting the direct adoption of southern accessions in the north. Consistent with this, Central Asian accessions have a faster life cycle potentially adaptive to both short growing season and reduced soil water availability, with reduced plant size and lower yield as tradeoffs. These accessions also have increased root:shoot ratio for drought adaptation, similar to findings in rice (Xu et al., 2015), alfalfa (Zhang et al., 2018), and chickpea (Kumar et al., 2012).

About accession sampling and climatic niche modeling, we recognize that not all samples have available spatial data, and we do not have samples from some parts of Asia. For example, while most samples of the SEA group were collected from Taiwan, Thailand, and Philippines, we do not have many samples from the supposed contact zone between SA and SEA (Bangladesh and Myanmar) or between SEA and EA (southern China). If more samples were available from these contact zones, the modeled niche space between SA and SEA and between SEA and EA would be even more similar than the current estimate, strengthening our hypothesis that niche similarity might facilitate the cultivation expansion. On the other hand, clear niche differentiation between SA and CA was evident despite the dense sampling near their contact zone. Based on the Köppen climate classification, South Asia could be roughly separated into two major zones, with the eastern zone slightly more similar to Southeast Asia (Figure 3-figure supplement 2). This partially explained the existence of some SEA accessions in the northeastern coast of India. While the SEA genetic group was named after the geographic region where most of its members were found in the present time, we recognize the possibility that it first occupied northeastern South Asia when it diverged from SA. In that case, the SA-SEA divergence time (4.7 to 11.3 thousand generations ago) might indicate the divergence between the two climate zones within South Asia rather than the expansion of mungbean into Southeast Asia, which may occur much later.

Conclusion

Our study demonstrates that mungbean's cultivation range expansion is associated with climatic conditions, which shaped the genetic diversity and contributed to adaptive differentiation among genetic groups. The climatic differences likely also resulted in farmers' differential emphasis on using it mainly as a grain or green manure crop, further intensifying the phenotypic diversification among regional mungbean accessions that could be used as an invaluable genetic resource for genetic improvement in the future.

Materials and Methods

Plant materials and SNP genotyping

A total of 290 cultivated mungbean (*V. radiata* var. *radiata*) accessions were provided by the Vavilov Institute (VIR). Most of the accessions are mainly landraces collected during 1910-1960 are considered these accessions as oldest cultivated mungbean collection from VIR (Burlyaeva et al., 2019). The term landrace, as we use it here, refers to locally adaptive accessions coming from the countries traditionally cultivating them, which also lacks modern genetic improvement. The complete list of materials can be found in Supplementary file 1. Genomic DNA was extracted from a single plant per accession using the QIAGEN Plant Mini DNA kit according to the manufacturer's instruction with minor modification of pre-warming the AP1 buffer to 65^{o}C and increasing the incubation time of the P3 buffer up to 2 hours on ice to increase DNA yield. DNA samples were sent to Diversity Arrays Technology Pty Ltd, Canberra, Australia for diversity array technology sequence (DArTseq) genotyping.

DArTseq data of 521 accessions from the Australian Diversity Panel (ADP) (Noble et al., 2018) and 297 accessions from the World Vegetable Center (WorldVeg) mini-core (Breria et al., 2020) were also included in this study. In total, our dataset contains more than one thousand accessions (1,092) and covers worldwide diversity of cultivated mungbean representing a wide range of variation in seed colour (Figure 1A). Sixteen wild mungbean (*V. radiata* var. *sublobata*) accessions were included as an outgroup. While all accessions used in this study have the country of origin information, only those from VIR have detailed longitude and latitude information. Therefore, for analyses connecting genetic information and detailed location (the isolation by distance analyses), only the VIR samples were used.

The major goal of this study is to investigate the patterns of population expansion and the underlying ecological causes instead of detailed haplotype analyses of specific genomic regions. For this goal, genomewide SNPs provide similar information as whole-genome sequencing, as have been shown in other species. Compared to other genotyping-by-sequencing technologies, DArTseq has the additional advantage of less missing data among loci or individuals, providing a more robust estimation of population structure.

SNP calling

Trimmomatic version 0.38 (Bolger et al., 2014) was used to remove adapters based on the manufacturer's adapter sequences. Reads for each accession were trimmed for low-quality bases with quality scores of $Q \leq 10$ using SolexaQA version 3.1.7.1 (Cox et al., 2010) and mapped to the mungbean reference genome (Vradiata_ver6, (Kang et al., 2014) using the Burrows-Wheeler Aligner (BWA) version 0.7.15 (Li and Durbin, 2009). Reads were then sorted and indexed using samtools version 1.4.1 (Li et al., 2009). We used Genome Analysis Toolkit (GATK) version 3.7-0-gcfedb67 (McKenna et al., 2010) to call all sites, including variant and invariant sites. We obtained 1,247,721 sites with a missing rate of < 10% and a minimum quality score of 30. SNP calling was performed using GATK (McKenna et al., 2010). Finally, we used VCFtools version 0.1.13 (Danecek et al., 2011) to remove SNPs with more than two alleles and 10% missing data, resulting in 34,469 filtered SNPs. To reduce non-independence caused by linkage disequilibrium (LD) among SNPs, SNPs were pruned based on a 50-SNP window with a step of 5 SNPs and r^2 threshold of 0.5 in PLINK (Purcell et al., 2007). This dataset of 10,359 LD-pruned SNPs (10% missing data) was applied for all analyses related to population genomics unless otherwise noted. For TreeMix that require LD-pruned SNPs with no missing dataset, we used 4,396 LD-pruned SNPs with no missing data.

Population genetics and differentiation analyses

Population structure was investigated based on 10,359 LD-pruned SNPs using ADMIXTURE (Alexander et al., 2009) with the number of clusters (K) ranging from 1 to 10. The analyses were run ten times for each K value, and cross-validation (CV) error was used to obtain the most probable K value for population structure analysis. ADMIXTURE plots were generated using "Pophelper" in R (Francis, 2017). Genetic groups of accessions were assigned based on ancestry coefficient $Q \geq 0.7$, otherwise the accession was considered admixed. The population structure

was also examined with principal component analysis (PCA). The neighbor-joining phylogenetic tree was calculated using TASSEL (Trait Analysis by aSSociation, Evolution and Linkage) software version 5.2.60 (Bradbury et al., 2007) and visualized using FigTree version 1.4.4 (http://tree.bio.ed.ac.uk/software/figtree/).

The relationships and gene flow among the four inferred genetic groups were further assessed by TreeMix version 1.12 (Pickrell and Pritchard, 2012) using 4,396 LD-pruned SNPs with no missing data. The analysis was run for 0 to 3 migration events with *V. radiata* var. *sublobata* as an outgroup with a block size of 20 SNPs to account for the effects of LD between SNPs. We estimated one as the optimal number of migration events using the "OptM" in R (Fitak, 2021). Bootstrap support for the resulting observed topology was obtained using 500 bootstrap replicates.

Nucleotide diversity (π) and genetic differentiation (d_{xy} and F_{ST}) were estimated in 10 kb windows with pixy version 1.2.7.beta1 (Korunes and Samuk, 2021) using all 1,247,721 invariant and variant sites. LD decay for each genetic group was estimated based on 34,469 non-LD-pruned SNPs using PopLDdecay (Zhang et al., 2019). The curves were fitted by a LOESS function and an LD decay plot was drawn using R.

To investigate the relation among inferred genetic groups, *f*3 and *f*4 statistics were computed based on filtered SNPs using ADMIXTOOLS version 7.0 (Patterson et al., 2012). The *f*3 statistic compares allele frequencies in two populations (A, B) and a target population C. In "outgroup *f*3 statistic", C is the outgroup and positive values represent the shared genetic drift between A and B. In "admixture *f*3 statistic", negative values indicate that the C is admixed from A and B. For *f*4 statistics, *f*4(A, B; C, D) measures the shared genetic drift between B populations and C and D after their divergence from outgroup A. A positive value indicates that the B population shares more alleles with D, and a negative value indicates that the B population shares more alleles with C. We used two Mb as a unit of block-jackknife resampling to compute standard errors. The Z-scores with absolute values greater than three are considered statistically significant.

To examine the role of geographic distance in shaping spatial genetic differentiation, Mantel tests with 1,000 permutations were performed for each of the ADMIXTURE-inferred genetic groups (separately for the groups defined by $Q \geq 0.7$ or $Q \geq 0.5$) using "ade4" in R.

Pairwise genetic distance between accessions was estimated based on all sites while the great circle geographic distance was determined using "fields" in R. In addition, the same analysis was conducted for southern and northern groups to examine if there was a south-north pattern of differentiation.

Based on the shape of the phylogenetic tree, we used fastsimcoal2 (Excoffier et al., 2021), which does not rely on whole-genome sequencing, to estimate the split time among genetic groups. Fifty accessions were randomly picked from each genetic group. Population size was allowed to change, and gene flow was allowed among populations. This analysis used all sites covered by the DArT tags (including monomorphic sites), and the mutation rate was set to $1x10^{-8}$ which was within the range of mutation rates used in eudicots (Barrera-Redondo et al., 2021; Zheng et al., 2022). The models were run using unfolded site frequency spectrum using the major allele in the wild progenitor population (*V. radiata* var. *sublobata*) as the ancestral allele. The model was run independently 100 times, each with 100,000 simulations. After obtaining the run with the highest likelihood, we performed parametric bootstrapping 100 times to obtain the 75% confidence intervals of each parameter based on the previous study of Gutaker et al. (2020).

Ecological niche modelling (ENM)

To understand whether the habitats of genetic groups are differentiated, 248 sampling sites (82 for East Asia, 45 for Southeast Asia, 49 for South Asia and 72 for Central Asia genetic groups), in combination with additional presence records obtained from the Global Biodiversity Information Facility (GBIF, https://www.gbif.org/), were used for the analysis. Using the longitude and latitude information, we extracted the Köppen climate zones (Köppen, 2011) using "kgc" in R (Bryant et al., 2017). After excluding zones with less than five samples, the remaining ten zones were grouped into six categories based on climate similarity: dry hot (BSh and BWh), dry cold (BSk and BWk), temperate dry summer (Csa), tropical savanna (Aw), Continental (Dwb and Dfb), and temperate wet summer (Cfa and Cwa). The former three are relatively dry environments.

Climate layers comprising monthly minimum, maximum, mean temperature, precipitation, and 19 bioclimatic variables were downloaded from the WorldClim database version 1.4 (Hijmans et al., 2005). All climate layers available from WorldClim were created

based on climate conditions recorded between 1960 and 1990 at a spatial resolution of 30 arc-seconds (approximately 1 km^2). To minimize redundancy and model overfitting, pairwise Pearson correlations between the 19 bioclimatic variables were calculated using ENMTools version 1.4.4 (Warren et al., 2010), excluding one of the two variables that has a correlation above 0.8 (Supplementary file 6). As a result, eight bioclimatic variables were used for all further analyses, including Bio1 (annual mean temperature), Bio2 (mean diurnal range), Bio3 (isothermality), Bio8 (mean temperature of wettest quarter), Bio12 (annual precipitation), Bio14 (precipitation of driest month), Bio15 (precipitation seasonality) and Bio19 (precipitation of coldest month). Bioclimatic variables were extracted for each occurrence point using "raster" in R (Hijmans, 2021). PCA and multivariate analysis of variance (MANOVA) were conducted to examine whether there was a significant habitat difference among genetic groups. Ecological niche modelling (ENM) was performed using MAXENT version 3.3.1 (Phillips et al., 2006) to predict the geographic distribution of suitable habitats for cultivated mungbean. The ENM analysis was run with a random seed, a convergence threshold of 5,000 and 10-fold cross-validation. As a measure of the habitat overlaps of the four genetic groups, pairwise of Schoener's D was calculated using ENMTools. The value ranges from 0 (no niche overlap) to 1 (niche complete overlap). In addition, we carried out the same analyses using monthly temperature and precipitation from May, July, and September.

Field evaluation

Among the 52 accessions used for laboratory experiments, phenotyping of 49 accessions was conducted at WorldVeg, Taiwan in 1984 and 2018 and at Crop Sciences Institute, National Agricultural Research Centre, Pakistan in 2015. The traits related to phenology (days to 50% flowering), reproduction (100 seed weight, pod length, pods per plant, 1000 seed weight, seeds yield per plant, and seeds per pod), and plant size (petiole length, plant height, plant height at flowering, plant height at maturity, primary leaf length, primary leaf width, terminal leaflet length, and terminal leaflet width) were included. Trait values were inverse normal transformed. The analysis of variance (ANOVA) was performed to test for inferred genetic groups differences for each trait using R software (version 4.1.0).

Drought phenotyping

A total of 52 accessions with ancestry coefficients Q ≥ 0.7 from three genetic groups (Southeast Asia, South Asia, and Central Asia) were selected for experiments of seedling-stage drought response. The experiment was laid out in a completely randomized design with three replicates of each accession under two treatments (control/drought). The experiment was conducted in two independent batches, and the whole experiment included 624 plants (52 accessions x 2 treatments x 3 plants per treatment x 2 batches).

Mungbean seeds were surface-sterilized with 10% bleach for 10 mins and rinsed with distilled water for three times. Seeds were treated with 70% ethanol for 5 mins and washed three times in distilled water. The sterilized seeds were germinated on wet filter paper in petri dishes for 3 days. The experiment was conducted in a 740FLED-2D plant growth chamber (HiPoint, Taiwan) at a temperature of 25 ± 1°C and 12 hours of photoperiod (light ratios of red: green: blue 3: 1: 1) with light intensity 350 µmol $m^{-2}s^{-1}$ and relative humidity at 60 ± 5%. The seedlings were then transplanted to a hydroponic system with half-strength Hoagland nutrient solution (Phytotechnology Laboratory, USA) and were grown for six days before drought stress started. The nutrient solution was changed on alternate days and the pH of the solution was adjusted to 6.0 with 1M KOH or 1M HCl.

For drought treatment, seedlings of mungbean were exposed to polyethylene glycol (PEG)-induced drought stress for five days. The solution of PEG6000 with an osmotic potential of -0.6 MPa was prepared by adding PEG6000 (Sigma-Aldrich, Germany) to the nutrient solution according to Michel and Kaufmann (1973), and pH was also adjusted to 6.0. The seedlings grown with the nutrient solution under the same environmental conditions were considered as controls.

At the end of the experiment, plants were evaluated for shoot dry weight (SDW) and root dry weight (RDW), measured on digital balance after oven-drying at 70°C for 48 hours. All traits were analysed by mixed-model ANOVA with the treatment (control/drought) and the genetic group as fixed effects. The models included accessions as a random effect nested within genetic groups and a random effect of batches. Tukey's test was conducted to compare genetic groups. All statistics were performed using JMP v3.0.0 (SAS Institute, 2016).

Q_{ST}-F_{ST} comparisons

For each trait, quantitative trait divergence (Q_{ST}) was calculated separately with respect to each treatment. Our root and shoot weight experiment used a selfed-progeny design, using the self-fertilized seeds from each accession as replicates, as recommended for partially inbred species (Goudet and Buchi, 2006). For the selfed-progeny design of inbred species, (Equation 1) $Q_{ST} = V_B / (V_B + V_{Fam})$, where V_B is the among-population variance component and V_{Fam} is the within-population among-family variance component (Goudet and Buchi, 2006). Variance components were estimated using a model with genetic groups, accessions nested within genetic groups, and batches as random factors. To accommodate the possibility that mungbean is not completely selfing, we also applied (Equation 2) $Q_{ST} = (1 + f)V_B / ((1 + f)V_B + 2V_{AW})$ (Goudet and Buchi, 2006), where f is the inbreeding coefficient (estimated by VCFtools as 0.8425), V_B is the among-population variance component, and V_{AW} is the additive genetic variance within genetic groups estimated by the kinship matrix using TASSEL software (Bradbury et al., 2007). The results and conclusions are similar to our previous version. The F_{ST} was calculated only using accessions in the phenotyping experiment.

Acknowledgements

We thank Chia-Yu Chen and Shang-Ying Tien for their assistance in sample preparation. C-RL was funded by 107-2923-B-002-004-MY3 and 110-2628-B-002-027 from the Ministry of Science and Technology, Taiwan. C-TT was funded by 107-2923-B-002-004-MY3 from the Ministry of Science and Technology, Taiwan. Y-PL was supported by 110-2313-B-125-001-MY3 from the Ministry of Science and Technology, Taiwan. RN and RS were funded by the Australian Center for International Agricultural Research (ACIAR) through the projects on International Mungbean Improvement Network (CIM-2014-079 and CROP-2019-144) and by the strategic long-term donors to the World Vegetable Center: Republic of China (Taiwan), UK aid from the UK government, United States Agency for International Development (USAID), Germany, Thailand, Philippines, Korea, and Japan. EBvW was supported by USDA Multistate Hatch NE1710. EBvW and MS were supported by Russian Scientific Fund Project No. 18-46-08001 and the Ministry of Science and Higher Education of the Russian Federation as part of World-class Research Center program: Advanced Digital Technologies (contract No. 075-15-2020-934 dated 17.11.2020). SN was supported by the Zumberge foundation.

Data Availability

Sequences generated in this study are available under NCBI BioProject PRJN809503. Accession names, GPS coordinates, and NCBI accession numbers of the Vavilov Institute accessions are available under Supplementary file 1. Plant trait data are available at Dryad https://doi.org/10.5061/dryad.d7wm37q3h. Sequences and accession information of the World Vegetable Centre mini-core and the Australian Diversity Panel collections were obtained from Breria et al. (2020) and Noble et al. (2018).

References

Alexander DH, Novembre J, Lange K. 2009. Fast model-based estimation of ancestry in unrelated individuals. *Genome Research* **19**:1655-1664. DOI: https://doi.org/10.1101/gr.094052.109

Annanepesov M, Bababekov HN. 2003. The khanates of khiva and kokand and the relations between the knanates and with other powers. In: Adle C, Habib I (Eds). *History of Civilizations of Central Asia, Volume 5: Development in Contrast, from the Sixteenth to the mid-Nineteenth Century*. Paris: UNESCO Publishing. p. 64-89.

Barrera-Redondo J, Sánchez-de la Vega G, Aguirre-Liguori JA, Castellanos-Morales G, Gutiérrez-Guerrero YT, Aguirre-Dugua X, Aguirre-Planter E, Tenaillon MI, Lira-Saade R, Eguiarte LE. 2021. The domestication of *Cucurbita argyrosperma* as revealed by the genome of its wild relative. *Horticulture Research* **8**:109. DOI: https://doi.org/10.1038/s41438-021-00544-9

Bolger AM, Lohse M, Usadel B. 2014. Trimmomatic: a flexible trimmer for Illumina sequence data. *Bioinformatics* **30**:2114-2120. DOI: https://doi.org/10.1093/bioinformatics/btu170

Bradbury PJ, Zhang Z, Kroon DE, Casstevens TM, Ramdoss Y, Buckler ES. 2007. TASSEL: software for association mapping of complex traits in diverse samples. *Bioinformatics* **23**:2633-2635. DOI: https://doi.org/10.1093/bioinformatics/btm308

Breria CM, Hsieh CH, Yen J-Y, Nair R, Lin C-Y, Huang S-M, Noble TJ, Schafleitner R. 2020. Population structure of the world vegetable center mungbean mini core collection and genome-wide association mapping of loci associated with variation of seed coat luster. *Tropical Plant Biology* **13**:1-12. DOI: https://doi.org/10.1007/s12042-019-09236-0

Bryant C, Wheeler NR, Rubel F, French RH. (2017). kgc: Köeppen-Geiger climatic zones. (Version R package version 1.0.0.2.). Retrieved from https://CRAN.R-project.org/package=kgc

Burlyaeva M, Vishnyakova M, Gurkina M, Kozlov K, Lee C-R, Ting C-T, Schafleitner R, Nuzhdin S, Samsonova M, von Wettberg E. 2019. Collections of mungbean [*Vigna radiata*) (L.) R. Wilczek] and urdbean [*V. mungo* (L.) Hepper] in Vavilov Institute (VIR): traits diversity and trends in the breeding process over the last 100 years. *Genetic Resources and Crop Evolution* **66**:767-781. DOI: https://doi.org/10.1007/s10722-019-00760-2

675 Castillo CC, Bellina B, Fuller DQ. 2016. Rice, beans and trade crops on the early maritime Silk
676 Route in Southeast Asia. *Antiquity* **90**:1255-1269. DOI:
677 https://doi.org/10.15184/aqy.2016.175
678 Chen L-T. 1980. A study of the systems of rotating crops in Chinese history 我國歷代輪種制度
679 之研究. *Bulletin of the Institute of History and Philology* **51**:281-313.
680 Cox MP, Peterson DA, Biggs PJ. 2010. SolexaQA: At-a-glance quality assessment of Illumina
681 second-generation sequencing data. *BMC Bioinformatics* **11**:485. DOI:
682 https://doi.org/10.1186/1471-2105-11-485
683 Danecek P, Auton A, Abecasis G, Albers CA, Banks E, DePristo MA, Handsaker RE, Lunter G,
684 Marth GT, Sherry ST, McVean G, Durbin R. 2011. The variant call format and VCFtools.
685 *Bioinformatics* **27**:2156-2158. DOI: https://doi.org/10.1093/bioinformatics/btr330
686 Dela Vina AC, Tomooka N. 1994. Genetic diversity in mungbean [*Vigna radiata* (L.) Wilczek]
687 based on two enzyme systems. *Philippine Journal of Crop Science* **19**:1-9.
688 Douglas C, Pratap A, Rao BH, Manu B, Dubey S, Singh P, Tomar R. 2020. Breeding Progress
689 and Future Challenges: Abiotic Stresses. In: Nair R M, Schafleitner R, Lee S-H (Eds).
690 *The Mungbean Genome*. Cham: Springer International Publishing. p. 81-96.
691 Dupuy PD. 2016. Bronze Age Central Asia. In: *The Oxford Handbook of Topics in Archaeology*:
692 Oxford University Press.
693 Excoffier L, Marchi N, Marques DA, Matthey-Doret R, Gouy A, Sousa VC. 2021. fastsimcoal2:
694 demographic inference under complex evolutionary scenarios. *Bioinformatics* **37**:4882-
695 4885. DOI: https://doi.org/10.1093/bioinformatics/btab468
696 Fitak RR. 2021. OptM: estimating the optimal number of migration edges on population trees
697 using Treemix. *Biology Methods and Protocols* **6**. DOI:
698 https://doi.org/10.1093/biomethods/bpab017
699 Francis RM. 2017. pophelper: an R package and web app to analyse and visualize population
700 structure. *Molecular ecology resources* **17**:27-32. DOI: https://doi.org/10.1111/1755-
701 0998.12509
702 Fuller DQ. 2007. Contrasting patterns in crop domestication and domestication rates: recent
703 archaeobotanical insights from the old world. *Annals of Botany* **100**:903-924. DOI:
704 https://doi.org/10.1093/aob/mcm048
705 Fuller DQ, Boivin N, Hoogervorst T, Allaby R. 2011. Across the Indian Ocean: the prehistoric
706 movement of plants and animals. *Antiquity* **85**:544-558. DOI:
707 10.1017/S0003598X00067934
708 Fuller DQ, Harvey EL. 2006. The archaeobotany of Indian pulses: identification, processing and
709 evidence for cultivation. *Environmental Archaeology* **11**:219-246. DOI:
710 https://doi.org/10.1179/174963106x123232
711 Goudet Jm, Buchi L. 2006. The effects of dominance, regular inbreeding and sampling design on
712 Q_{ST}, an estimator of population differentiation for quantitative traits. *Genetics* **172**:1337-
713 1347. DOI: https://doi.org/10.1534/genetics.105.050583
714 Gutaker RM, Groen SC, Bellis ES, Choi JY, Pires IS, Bocinsky RK, Slayton ER, Wilkins O,
715 Castillo CC, Negrão S, Oliveira MM, Fuller DQ, Guedes JAdA, Lasky JR, Purugganan
716 MD. 2020. Genomic history and ecology of the geographic spread of rice. *Nature Plants*
717 **6**:492-502. DOI: https://doi.org/10.1038/s41477-020-0659-6
718 Gwag J-G, Dixit A, Park Y-J, Ma K-H, Kwon S-J, Cho G-T, Lee G-A, Lee S-Y, Kang H-K, Lee
719 S-H. 2010. Assessment of genetic diversity and population structure in mungbean. *Genes*
720 *& Genomics* **32**:299-308. DOI: https://doi.org/10.1007/s13258-010-0014-9

721 Ha J, Lee S-H. 2019. Mung bean (*Vigna radiata* (L.) R. Wilczek) breeding. In: Al-Khayri J M,
722 Jain S M, Johnson D V (Eds). *Advances in Plant Breeding Strategies: Legumes: Volume*
723 *7*. Cham: Springer International Publishing. p. 371-407.
724 Ha J, Satyawan D, Jeong H, Lee E, Cho K-H, Kim MY, Lee S-H. 2021. A near-complete genome
725 sequence of mungbean (*Vigna radiata* L.) provides key insights into the modern breeding
726 program. *Plant Genome* **14**:e20121. DOI: https://doi.org/10.1002/tpg2.20121
727 Herniter IA, Muñoz-Amatriaín M, Close TJ. 2020. Genetic, textual, and archeological evidence
728 of the historical global spread of cowpea (*Vigna unguiculata* [L.] Walp.). *Legume Science*
729 **2**:e57. DOI: https://doi.org/10.1002/leg3.57
730 Hijmans R. (2021). Raster: geographic data analysis and modeling (Version R package version
731 3.4-13). Retrieved from https://CRAN.R-project.org/package=raster
732 Hijmans RJ, Cameron SE, Parra JL, Jones PG, Jarvis A. 2005. Very high resolution interpolated
733 climate surfaces for global land areas. *International Journal of Climatology* **25**:1965-1978.
734 DOI: https://doi.org/10.1002/joc.1276
735 Islam ASMF, Blair MW. 2018. Molecular characterization of mung bean germplasm from the
736 USDA core collection using newly developed KASP-based SNP markers. *Crop Science*
737 **58**:1659-1670. DOI: https://doi.org/10.2135/cropsci2018.01.0044
738 Jeong C, Balanovsky O, Lukianova E, Kahbatkyzy N, Flegontov P, Zaporozhchenko V, Immel
739 A, Wang C-C, Ixan O, Khussainova E, Bekmanov B, Zaibert V, Lavryashina M,
740 Pocheshkhova E, Yusupov Y, Agdzhoyan A, Koshel S, Bukin A, Nymadawa P,
741 Turdikulova S, Dalimova D, Churnosov M, Skhalyakho R, Daragan D, Bogunov Y,
742 Bogunova A, Shtrunov A, Dubova N, Zhabagin M, Yepiskoposyan L, Churakov V,
743 Pislegin N, Damba L, Saroyants L, Dibirova K, Atramentova L, Utevska O, Idrisov E,
744 Kamenshchikova E, Evseeva I, Metspalu M, Outram AK, Robbeets M, Djansugurova L,
745 Balanovska E, Schiffels S, Haak W, Reich D, Krause J. 2019. The genetic history of
746 admixture across inner Eurasia. *Nature Ecology & Evolution* **3**:966-976. DOI:
747 https://doi.org/10.1038/s41559-019-0878-2
748 Jones H, Leigh FJ, Mackay I, Bower MA, Smith LMJ, Charles MP, Jones G, Jones MK, Brown
749 TA, Powell W. 2008. Population-based resequencing reveals that the flowering time
750 adaptation of cultivated barley originated east of the fertile crescent. *Molecular Biology*
751 *and Evolution* **25**:2211-2219. DOI: https://doi.org/10.1093/molbev/msn167
752 Jones H, Lister DL, Cai D, Kneale CJ, Cockram J, Peña-Chocarro L, Jones MK. 2016. The trans-
753 Eurasian crop exchange in prehistory: Discerning pathways from barley phylogeography.
754 *Quaternary International* **426**:26-32. DOI: https://doi.org/10.1016/j.quaint.2016.02.029
755 Jones M, Hunt H, Lightfoot E, Lister D, Liu X, Motuzaite-Matuzeviciute G. 2011. Food
756 globalization in prehistory. *World Archaeology* **43**:665-675. DOI:
757 https://doi.org/10.1080/00438243.2011.624764
758 Kang YJ, Kim SK, Kim MY, Lestari P, Kim KH, Ha BK, Jun TH, Hwang WJ, Lee T, Lee J,
759 Shim S, Yoon MY, Jang YE, Han KS, Taeprayoon P, Yoon N, Somta P, Tanya P, Kim
760 KS, Gwag JG, Moon JK, Lee YH, Park BS, Bombarely A, Doyle JJ, Jackson SA,
761 Schafleitner R, Srinives P, Varshney RK, Lee SH. 2014. Genome sequence of mungbean
762 and insights into evolution within *Vigna* species. *Nature Communications* **5**:5443. DOI:
763 https://doi.org/10.1038/ncomms6443
764 Kim SK, Nair RM, Lee J, Lee SH. 2015. Genomic resources in mungbean for future breeding
765 programs. *Frontiers in Plant Science* **6**:626. DOI:
766 https://doi.org/10.3389/fpls.2015.00626

767 Kingwell-Banham E, Petrie CA, Fuller DQ. 2015. Early agriculture in South Asia. In: Goucher
768 C, Barker G (Eds). *The Cambridge World History: Volume 2: A World with Agriculture,*
769 *12,000 BCE–500 CE* (Vol. 2). Cambridge: Cambridge University Press. p. 261-288.
770 Kistler L, Maezumi SY, Souza JGd, Przelomska NAS, Costa FM, Smith O, Loiselle H, Ramos-
771 Madrigal J, Wales N, Ribeiro ER, Morrison RR, Grimaldo C, Prous AP, Arriaza B,
772 Gilbert MTP, Freitas FdO, Allaby RG. 2018. Multiproxy evidence highlights a complex
773 evolutionary legacy of maize in South America. *Science* **362**:1309-1313. DOI:
774 https://doi.org/doi:10.1126/science.aav0207
775 Kohl PL. 2007. Entering a Sown World of Irrigation Agriculture – From the Steppes to Central
776 Asia and Beyond: Processes of Movement, Assimilation, and Transformation into the
777 "Civilized" World East of Sumer. In: Kohl P L (Ed). *The Making of Bronze Age Eurasia*.
778 Cambridge: Cambridge University Press. p. 182-243.
779 Kohl PL, Lyonnet B. 2008. By land and by sea: The circulation of materials and peoples, ca.
780 3500-1800 B.C. In: Olijdam E, Spoor R H (Eds). *Intercultural Relations between South*
781 *and Southwest Asia. Studies in Commemoration of E.C.L. During Caspers (1934–1996).*
782 *BAR International Series 1826*. Oxford: Archaeopress. p. 29-42.
783 Köppen W. 2011. The thermal zones of the Earth according to the duration of hot, moderate and
784 cold periods and to the impact of heat on the organic world. *Meteorologische Zeitschrif*
785 **20**:351-360. DOI: https://doi.org/10.1127/0941-2948/2011/105
786 Korunes KL, Samuk K. 2021. pixy: Unbiased estimation of nucleotide diversity and divergence
787 in the presence of missing data. *Molecular Ecology Resources* **21**:1359-1368. DOI:
788 https://doi.org/10.1111/1755-0998.13326
789 Kumar N, Nandwal AS, Waldia RS, Singh S, Devi S, Sharma KD, Kumar A. 2012. Drought
790 tolerance in chickpea as evaluated by root characteristics, plant water status, membrane
791 integrity and chlorophyll fluorescence techniques. *Experimental Agriculture* **48**:378-387.
792 DOI: https://doi.org/10.1017/S0014479712000063
793 Lamberg-Karlovsky CC. 2002. Archaeology and language: The Indo-Iranians. *Current*
794 *Anthropology* **43**:63-88. DOI: https://doi.org/10.1086/324130
795 Lee CR, Svardal H, Farlow A, Exposito-Alonso M, Ding W, Novikova P, Alonso-Blanco C,
796 Weigel D, Nordborg M. 2017. On the post-glacial spread of human commensal
797 *Arabidopsis thaliana*. *Nature Communications* **8**:14458. DOI:
798 https://doi.org/10.1038/ncomms14458
799 Li H, Durbin R. 2009. Fast and accurate short read alignment with Burrows-Wheeler transform.
800 *Bioinformatics* **25**:1754-1760. DOI: https://doi.org/10.1093/bioinformatics/btp324
801 Li H, Handsaker B, Wysoker A, Fennell T, Ruan J, Homer N, Marth G, Abecasis G, Durbin R,
802 Subgroup GPDP. 2009. The Sequence Alignment/Map format and SAMtools.
803 *Bioinformatics* **25**:2078-2079. DOI: https://doi.org/10.1093/bioinformatics/btp352
804 Lin Y-P, Chen H-W, Yeh P-M, Anand SS, Lin J, Li J, Noble T, Nair R, Schafleitner R,
805 Samsonova M, Bishop-von-Wettberg E, Nuzhdin S, Ting C-T, Lawn RJ, Lee C-R. 2022.
806 Distinct selection signatures during domestication and improvement in crops: a tale of
807 two genes in mungbean. *bioRxiv*. DOI: https://doi.org/10.1101/2022.09.08.506689
808 Lister DL, Jones H, Oliveira HR, Petrie CA, Liu X, Cockram J, Kneale CJ, Kovaleva O, Jones
809 MK. 2018. Barley heads east: Genetic analyses reveal routes of spread through diverse
810 Eurasian landscapes. *PLOS ONE* **13**:e0196652. DOI:
811 https://doi.org/10.1371/journal.pone.0196652

812 Liu X, Jones PJ, Motuzaite Matuzeviciute G, Hunt HV, Lister DL, An T, Przelomska N, Kneale
813 CJ, Zhao Z, Jones MK. 2019. From ecological opportunism to multi-cropping: Mapping
814 food globalisation in prehistory. *Quaternary Science Reviews* **206**:21-28. DOI:
815 https://doi.org/10.1016/j.quascirev.2018.12.017
816 Lombard P. 2020. The Oxus civilization/BMAC and its interaction with the Arabian Gulf. A
817 review of the evidences. In: Lyonnet; B, Dubova N (Eds). *The World of the Oxus*
818 *Civilization, Routledge* p. 607-634.
819 Lyonnet B. 2005. Another possible interpretation of the Bactro-Margiana culture (BMAC) of
820 Central Asia: The tin Trade. In: Jarrige C, Lefevre V (Eds). *South Asian Archaeology*
821 *Vol. 1 Prehistory*: Paris: Editions Recherche sur les Civilisations. p. 191-200.
822 McKenna A, Hanna M, Banks E, Sivachenko A, Cibulskis K, Kernytsky A, Garimella K,
823 Altshuler D, Gabriel S, Daly M, DePristo MA. 2010. The Genome Analysis Toolkit: a
824 MapReduce framework for analyzing next-generation DNA sequencing data. *Genome*
825 *Research* **20**:1297-1303. DOI: https://doi.org/10.1101/gr.107524.110
826 Meyer RS, Purugganan MD. 2013. Evolution of crop species: genetics of domestication and
827 diversification. *Nature Reviews Genetics* **14**:840-852. DOI:
828 https://doi.org/10.1038/nrg3605
829 Michel BE, Kaufmann MR. 1973. The osmotic potential of polyethylene glycol 6000. *Plant*
830 *Physiology* **51**:914-916. DOI: https://doi.org/10.1104/pp.51.5.914
831 Miller NF. 1999. Agricultural development in western Central Asia in the Chalcolithic and
832 Bronze Ages. *Vegetation History and Archaeobotany* **8**:13-19. DOI:
833 https://doi.org/10.1007/BF02042837
834 Mishra GP, Dikshit HK, Tripathi K, Aski MS, Pratap A, Dasgupta U, Nair RM, Gupta S. 2022.
835 Mungbean Breeding. In: Yadava D K, Dikshit H K, Mishra G P, Tripathi S (Eds).
836 *Fundamentals of Field Crop Breeding*. Singapore: Springer Nature Singapore. p. 1097-
837 1149.
838 Nair R, Schreinemachers P. 2020. Global status and economic importance of mungbean. In: Nair
839 R, Schafleitner R, Lee S-H (Eds). *The Mungbean Genome*. Berlin: Springer International
840 Publishing. p. 1-8.
841 Noble TJ, Tao Y, Mace ES, Williams B, Jordan DR, Douglas CA, Mundree SG. 2018.
842 Characterization of linkage disequilibrium and population structure in a mungbean
843 diversity panel. *Frontiers in Plant Science* **8**:2102. DOI:
844 https://doi.org/10.3389/fpls.2017.02102
845 Patterson N, Moorjani P, Luo Y, Mallick S, Rohland N, Zhan Y, Genschoreck T, Webster T,
846 Reich D. 2012. Ancient admixture in human history. *Genetics* **192**:1065-1093. DOI:
847 https://doi.org/10.1534/genetics.112.145037
848 Phillips SJ, Anderson RP, Schapire RE. 2006. Maximum entropy modeling of species geographic
849 distributions. *Ecological Modelling* **190**:231-259. DOI:
850 https://doi.org/10.1016/j.ecolmodel.2005.03.026
851 Pickrell JK, Pritchard JK. 2012. Inference of population splits and mixtures from genome-wide
852 allelefrequency data. *PLOS Genetics* **8**:e1002967. DOI:
853 https://doi.org/10.1371/journal.pgen.1002967
854 Pratap A, Gupta S, Basu PS, Tomar R, Dubey S, Rathore M, Prajapati US, Singh P, Kumari G.
855 2019. Towards development of climate smart mungbean: challenges and opportunities.
856 In: Kole C (Ed). *Genomic Designing of Climate-Smart Pulse Crops*. Chamsford: Springer
857 International Publishing. p. 235-264.

858 Purcell S, Neale B, Todd-Brown K, Thomas L, Ferreira MAR, Bender D, Maller J, Sklar P, de
859 Bakker PIW, Daly MJ, Sham PC. 2007. PLINK: A tool set for whole-genome association
860 and population-based linkage analyses. *The American Journal of Human Genetics*
861 **81**:559-575. DOI: https://doi.org/10.1086/519795
862 Rani S, Schreinemachers P, Kuziyev B. 2018. Mungbean as a catch crop for dryland systems in
863 Pakistan and Uzbekistan: A situational analysis. *Cogent Food & Agriculture* **4**:1499241.
864 DOI: https://doi.org/10.1080/23311932.2018.1499241
865 Sandhu K, Singh A. 2021. Strategies for the utilization of the USDA mung bean germplasm
866 collection for breeding outcomes. *Crop Science* **61**:422-442. DOI:
867 https://doi.org/10.1002/csc2.20322
868 Sangiri C, Kaga A, Tomooka N, Vaughan D, Srinives P. 2007. Genetic diversity of the mungbean
869 (*Vigna radiata*, Leguminosae) genepool on the basis of microsatellite analysis. *Australian*
870 *Journal of Botany* **55**:837-847. DOI: https://doi.org/10.1071/BT07105
871 Sokolkova A, Burlyaeva M, Valiannikova T, Vishnyakova M, Schafleitner R, Lee C-R, Ting C-
872 T, Nair RM, Nuzhdin S, Samsonova M, von Wettberg E. 2020. Genome-wide association
873 study in accessions of the mini-core collection of mungbean (*Vigna radiata*) from the
874 World Vegetable Gene Bank (Taiwan). *BMC Plant Biology* **20**:363. DOI:
875 https://doi.org/10.1186/s12870-020-02579-x
876 Spengler RN. 2015. Agriculture in the Central Asian Bronze Age. *Journal of World Prehistory*
877 **28**:215-253. DOI: https://doi.org/10.1007/s10963-015-9087-3
878 Spengler RN, Cerasetti B, Tengberg M, Cattani M, Rouse LM. 2014a. Agriculturalists and
879 pastoralists: Bronze Age economy of the Murghab alluvial fan, southern Central Asia.
880 *Vegetation History and Archaeobotany* **23**:805-820. DOI:
881 https://doi.org/10.1007/s00334-014-0448-0
882 Spengler RN, de Nigris I, Cerasetti B, Carra M, Rouse LM. 2018a. The breadth of dietary
883 economy in Bronze Age Central Asia: Case study from Adji Kui 1 in the Murghab region
884 of Turkmenistan. *Journal of Archaeological Science: Reports* **22**:372-381. DOI:
885 https://doi.org/10.1016/j.jasrep.2016.03.029
886 Spengler RN, Frachetti MD, Doumani PN. 2014b. Late Bronze Age agriculture at Tasbas in the
887 Dzhungar Mountains of eastern Kazakhstan. *Quaternary International* **348**:147-157. DOI:
888 https://doi.org/10.1016/j.quaint.2014.03.039
889 Spengler RN, Maksudov F, Bullion E, Merkle A, Hermes T, Frachetti M. 2018b. Arboreal crops
890 on the medieval Silk Road: Archaeobotanical studies at Tashbulak. *PLOS ONE*
891 **13**:e0201409. DOI: https://doi.org/10.1371/journal.pone.0201409
892 Spengler RN, Miller NF, Neef R, Tourtellotte PA, Chang C. 2017. Linking agriculture and
893 exchange to social developments of the Central Asian Iron Age. *Journal of*
894 *Anthropological Archaeology* **48**:295-308. DOI:
895 https://doi.org/10.1016/j.jaa.2017.09.002
896 Spengler RN, Tang L, Nayak A, Boivin N, Olivieri LM. 2021. The southern Central Asian
897 mountains as an ancient agricultural mixing zone: new archaeobotanical data from
898 Barikot in the Swat valley of Pakistan. *Vegetation History and Archaeobotany* **30**:463-
899 476. DOI: https://doi.org/10.1007/s00334-020-00798-8
900 Stevens CJ, Murphy C, Roberts R, Lucas L, Silva F, Fuller DQ. 2016. Between China and South
901 Asia: A Middle Asian corridor of crop dispersal and agricultural innovation in the Bronze
902 Age. *The Holocene* **26**:1541-1555. DOI: https://doi.org/10.1177/0959683616650268

903 Takahashi Y, Kongjaimun A, Muto C, Kobayashi Y, Kumagai M, Sakai H, Satou K, Teruya K,
904 Shiroma A, Shimoji M, Hirano T, Isemura T, Saito H, Baba-Kasai A, Kaga A, Somta P,
905 Tomooka N, Naito K. 2020. Same locus for non-shattering seed pod in two independently
906 domesticated legumes, *Vigna angularis* and *Vigna unguiculata*. *Frontiers in Genetics*
907 **11**:748. DOI: https://doi.org/10.3389/fgene.2020.00748
908 The 1001 Genomes Consortium. 2016. 1,135 Genomes reveal the global pattern of polymorphism
909 in *Arabidopsis thaliana*. *Cell* **166**:481-491. DOI:
910 https://doi.org/10.1016/j.cell.2016.05.063
911 Tomooka N, Lairungreang C, Nakeeraks P, Egawa Y, Thavarasook C. 1992. Center of genetic
912 diversity and dissemination pathways in mung bean deduced from seed protein
913 electrophoresis. *Theoretical and Applied Genetics* **83**:289-293. DOI:
914 https://doi.org/10.1007/BF00224273
915 Van der Veen M, Morales J. 2015. The Roman and Islamic spice trade: New archaeological
916 evidence. *Journal of Ethnopharmacology* **167**:54-63. DOI:
917 https://doi.org/10.1016/j.jep.2014.09.036
918 Vir R, Lakhanpaul S, Malik S, Umdale S, Bhat KV. 2016. Utilization of germplasm for the
919 genetic improvement of mung bean [*Vigna radiata* (L.) Wilczek]: The constraints and the
920 opportunities. In: Rajpal V R, Rao S R, Raina S N (Eds). *Gene Pool Diversity and Crop*
921 *Improvement: Volume 1*. Cham: Springer International Publishing. p. 367-391.
922 Warren DL, Glor RE, Turelli M. 2010. ENMTools: a toolbox for comparative studies of
923 environmental niche models. *Ecography* **33**:607-611. DOI:
924 https://doi.org/10.1111/j.1600-0587.2009.06142.x
925 Xu W, Cui K, Xu A, Nie L, Huang J, Peng S. 2015. Drought stress condition increases root to
926 shoot ratio via alteration of carbohydrate partitioning and enzymatic activity in rice
927 seedlings. *Acta Physiologiae Plantarum* **37**:9. DOI: https://doi.org/10.1007/s11738-014-
928 1760-0
929 Zhang C, Dong SS, Xu JY, He WM, Yang TL. 2019. PopLDdecay: a fast and effective tool for
930 linkage disequilibrium decay analysis based on variant call format files. *Bioinformatics*
931 **35**:1786-1788. DOI: https://doi.org/10.1093/bioinformatics/bty875
932 Zhang C, Shi S, Wang B, Zhao J. 2018. Physiological and biochemical changes in different
933 drought-tolerant alfalfa (*Medicago sativa* L.) varieties under PEG-induced drought stress.
934 *Acta Physiologiae Plantarum* **40**:25. DOI: https://doi.org/10.1007/s11738-017-2597-0
935 Zheng X, Wang T, Cheng T, Zhao L, Zheng X, Zhu F, Dong C, Xu J, Xie K, Hu Z, Yang L, Diao
936 Y. 2022. Genomic variation reveals demographic history and biological adaptation of the
937 ancient relictual, lotus (*Nelumbo* Adans.). *Horticulture Research* **9**:uhac029. DOI:
938 https://doi.org/10.1093/hr/uhac029

939

Supplementary note. Text analysis and translation of ancient Chinese texts regarding mungbean

Qimin Yaoshu (齊民要術, about 544 AD)

Qimin Yaoshu, compiled by Sixie Jia (賈思勰), is one of the earliest and most complete agricultural sources in China, detailing agricultural techniques near the lower reaches of Yellow River at that era. This is the earliest record of mungbean in China, demonstrating mungbean has reached northern China at that time and is consistent with our estimates of population divergence time. The popularity of mungbean is demonstrated by it being mentioned multiple times under different contexts, most notably as a green manure:

「若糞不可得者，五六月中，穊種菉豆，至七月、八月，犁掩殺之。如以糞糞田，則良美與糞不殊，又省功力。」

Translation: "Should feces be unavailable, during May and June one could grow mungbean. Until July or August, one could plow mungbean plants into the soil. This is equivalent to using feces to manure the land. This is as good as using feces and saves efforts."

Notice that the months used in ancient China are slightly different from the Gregorian calendar.

Xiangshan Yelu (湘山野錄, 1068-1077 AD)

Xiangshan Yelu was written by a monk, Wen-Ying (文瑩), recording anecdotes during that era. Its records about the Emperor Zhenzong of Song (宋真宗, 968-1022 AD) detailed the phenotypes of Indian mungbean at that time:

「真宗深念稼穡，聞占城稻耐旱、西天綠豆子多而粒大，各遣使以珍貨求其種。占城得種二十石，至今在處播之。西天中印土得菉豆種二石，不知今之菉豆是否？」

Translation: "Zhenzong of Song deeply concerned about agriculture. He heard Champa rice being drought tolerant and mungbean from India produce numerous and large seeds. Diplomats were sent to exchange the seeds with treasure. Twenty dans of Champa rice were obtained and propagated everywhere. Two dans of mungbean were obtained from India, but it is unclear whether the mungbean today descended from these."

"Dan" (石) is a unit of volume in ancient China and is called "Koku" in Japanese. The exact amount varied with time.

The texts provide us with two pieces of important information. First, mungbean from South Asia (likely also includes the SEA genetic groups if accessions near eastern India and Bangladesh were included) at that time had higher yield and larger seeds than native mungbean accessions in northern China, consistent with our results on trait divergence. Second, compared to the clear success of Champa rice in China, it was unclear whether those southern accessions had prospered in northern China, likely suggesting an unsuccessful introduction of southern high-yield and large-seeded accessions to the north.

Tiangong Kaiwu (天工開物, 1637 AD)

Tiangong Kaiwu is a famous Chinese encyclopedia compiled by Song Yingxing (宋應星). While it mostly covers technologies at that time, a section about agricultural practices covers mungbean:

「綠豆必小暑方種，未及小暑而種，則其苗蔓延數尺，結莢甚稀。若過期至於處暑，則隨時開花結莢，顆粒亦少。」

Translation: “Mungbean must be sown at or after Xiaoshu (Gregorian 7-8 July). Being sown before Xiaoshu, mungbean stems would spread for meters with few pods set. Being sown as late as Chushu (Gregorian 23-24 August), the plants would flower and set pods at any time, also with low yield.”

As a short-day plant, being sown too early when the days are too long, mungbean would have mostly vegetative growth. Being sown too late when the days are too short, flowering would be induced too quickly before sufficient vegetative development. In addition to our results that short-season accessions were favored in the north due to the requirement for drought escape, this source provides us with another support that mungbean could only be sown in a narrow time window due to daylength requirement. Given the autumn frost damage in the north, not being able to be sown earlier restricts the growing season length in the north, limiting the adoption of southern long-season accessions.

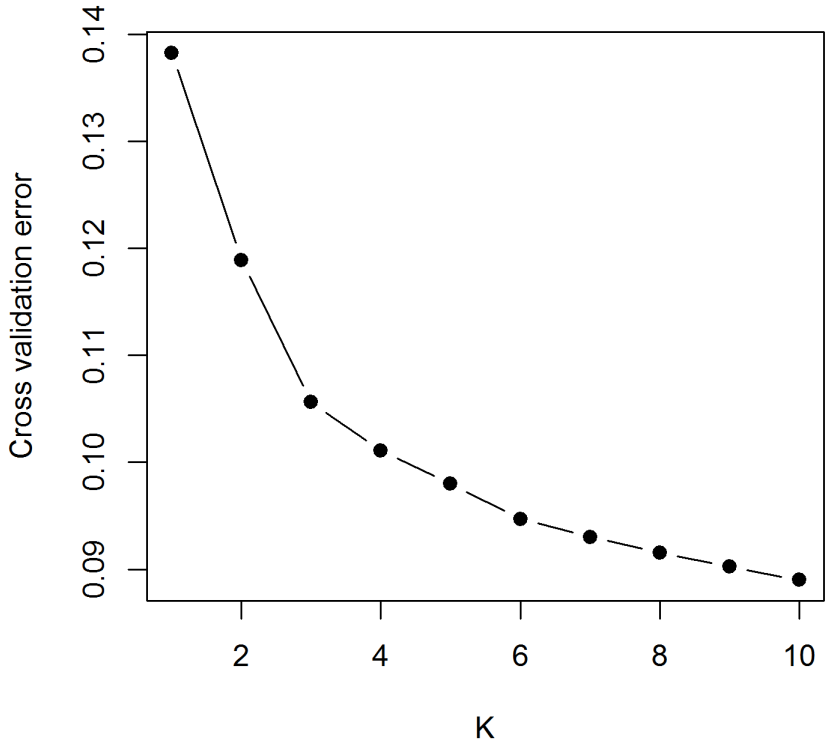

998 **Figure 1-figure supplement 1.** Cross-validation (CV) errors of ADMIXTURE. Means of CV errors
999 were calculated based on K values ranging 1 to 10 with 10 independent runs.

1000

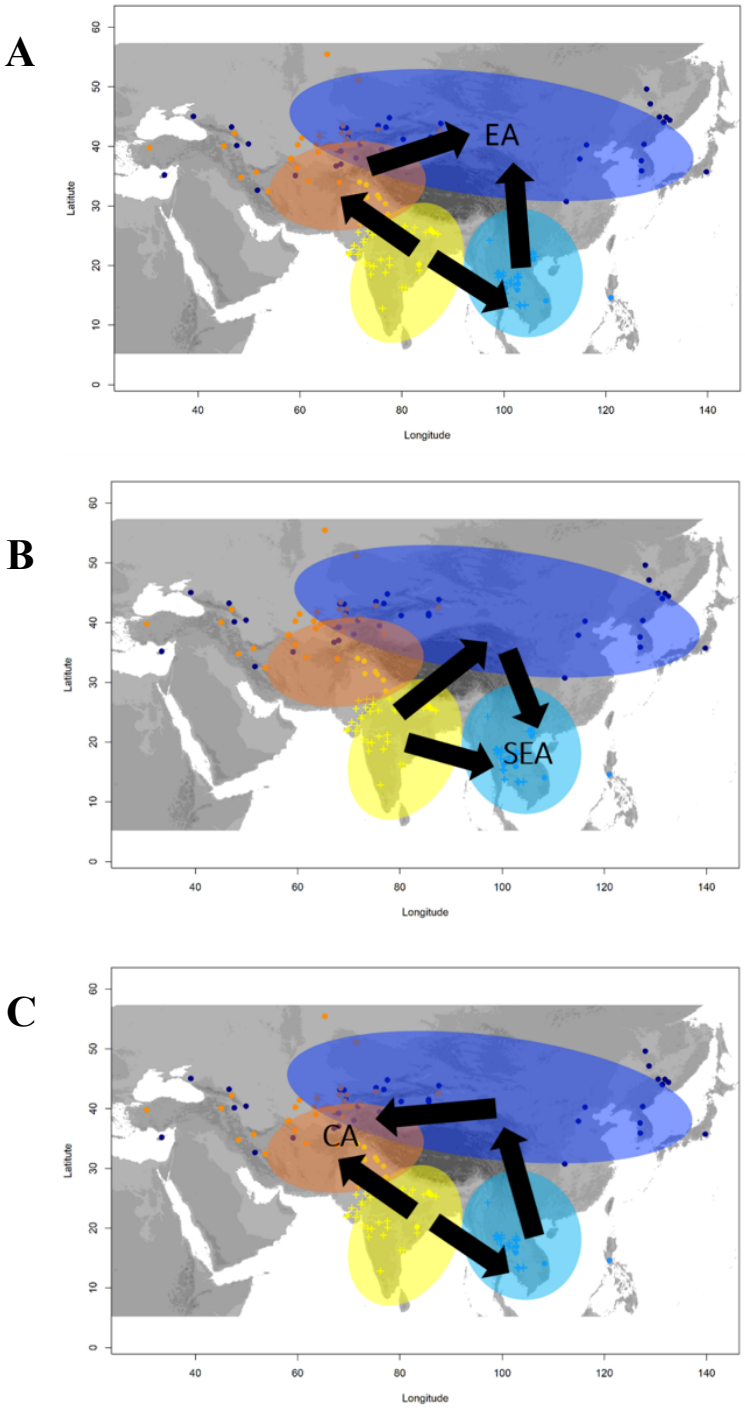

Figure 2-figure supplement 1. Schematic representation to investigate presence of admixture in a target population from two source populations using admixture f3-statistics. (A) f3(EA; SEA, CA), (B) f3(SEA; SA, EA) and (C) f3(CA; EA, SA). Coloured circles indicate the geographic area occupied by distinct genetic groups. Arrows indicates the possible direction of expansion and admixture among populations.

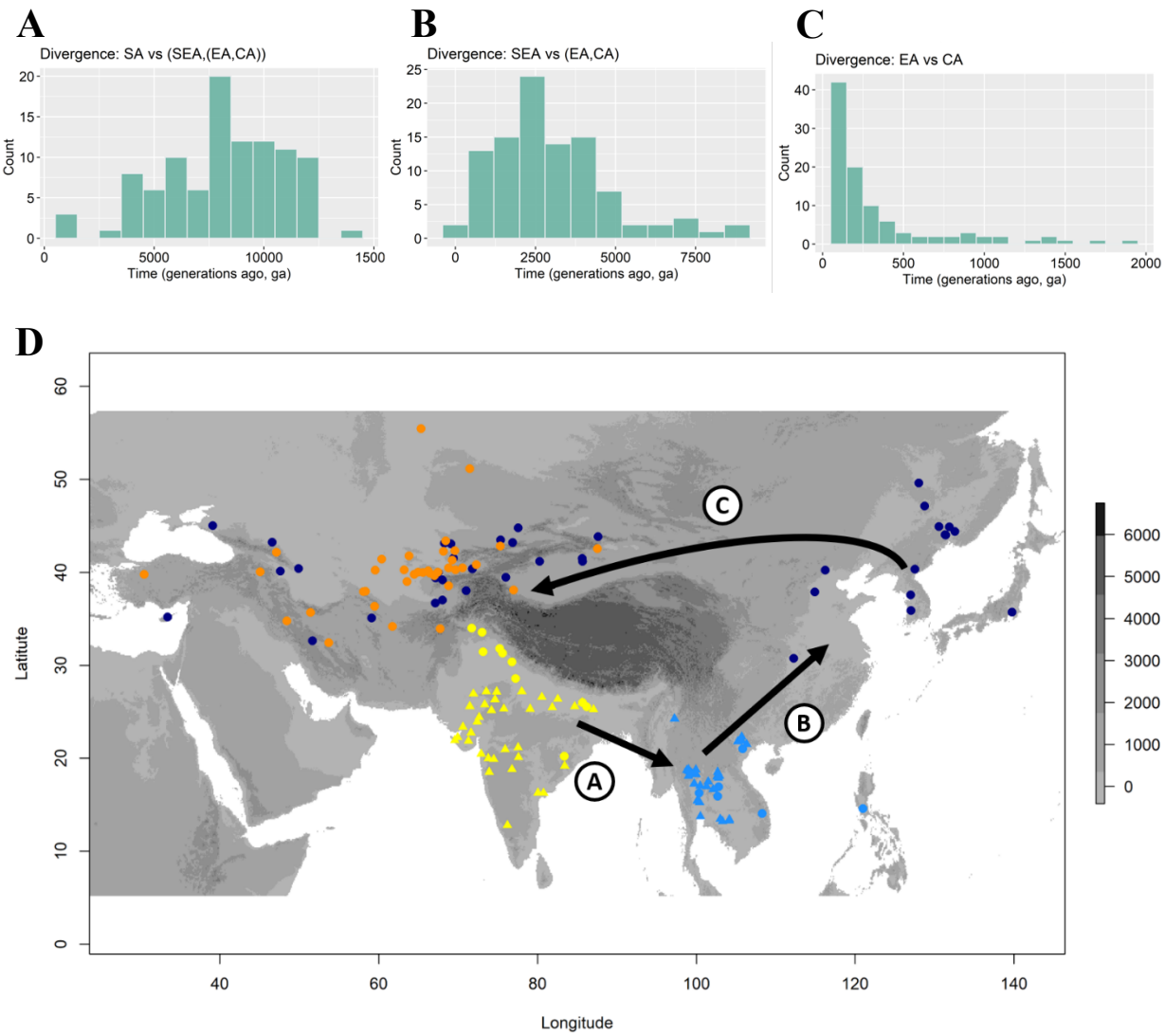

Figure 2-figure supplement 2. Estimates of divergence time and inferred mungbean movement over time across Asia. The histograms of the divergence times represent (A) split time between SA and (SEA,(EA,CA)), (B) split time between SEA and (EA,CA), and (C) split time between EA and CA. (D) Geographic distribution of mungbean accessions and proposed mungbean spread routes. Exact locations for VIR accessions (filled circle) and GBIF records (filled triangle) are provided. Each accession was coloured the same as an inferred genetic group using ADMIXTURE in Figure 1. Arrow indicates the possible expansion directions. The map was shaded as a gray colour representing altitude (meters above sea level).

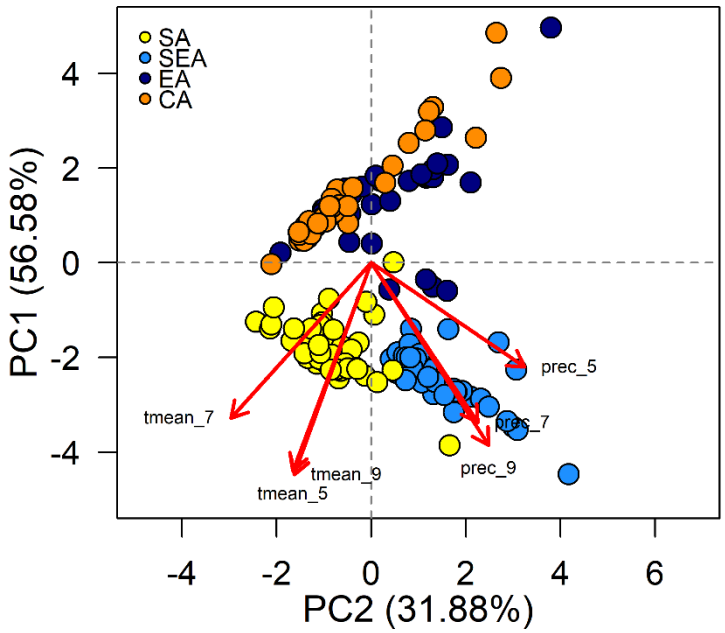

Figure 3-figure supplement 1. Principal component analysis (PCA) of the growing season climatic data including temperature and precipitation of May, July and September. Samples are coloured according to four inferred genetic groups, as indicated in the legend.

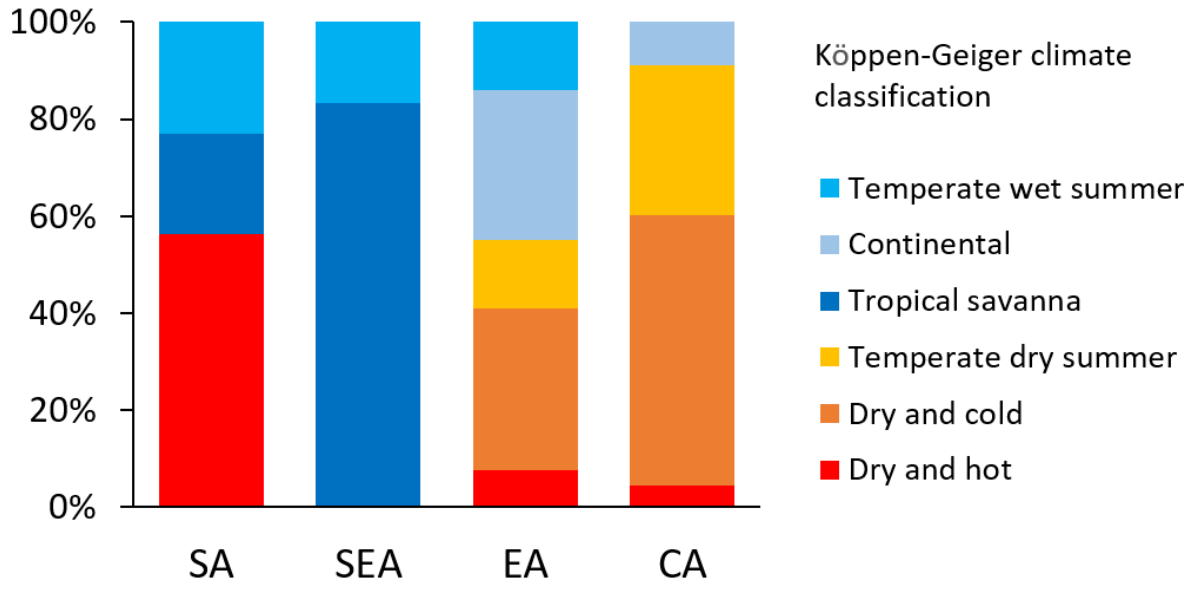

Figure 3-figure supplement 2. The distribution of accessions in major climate zones according to the Köppen climate classification (Köppen, 2011).

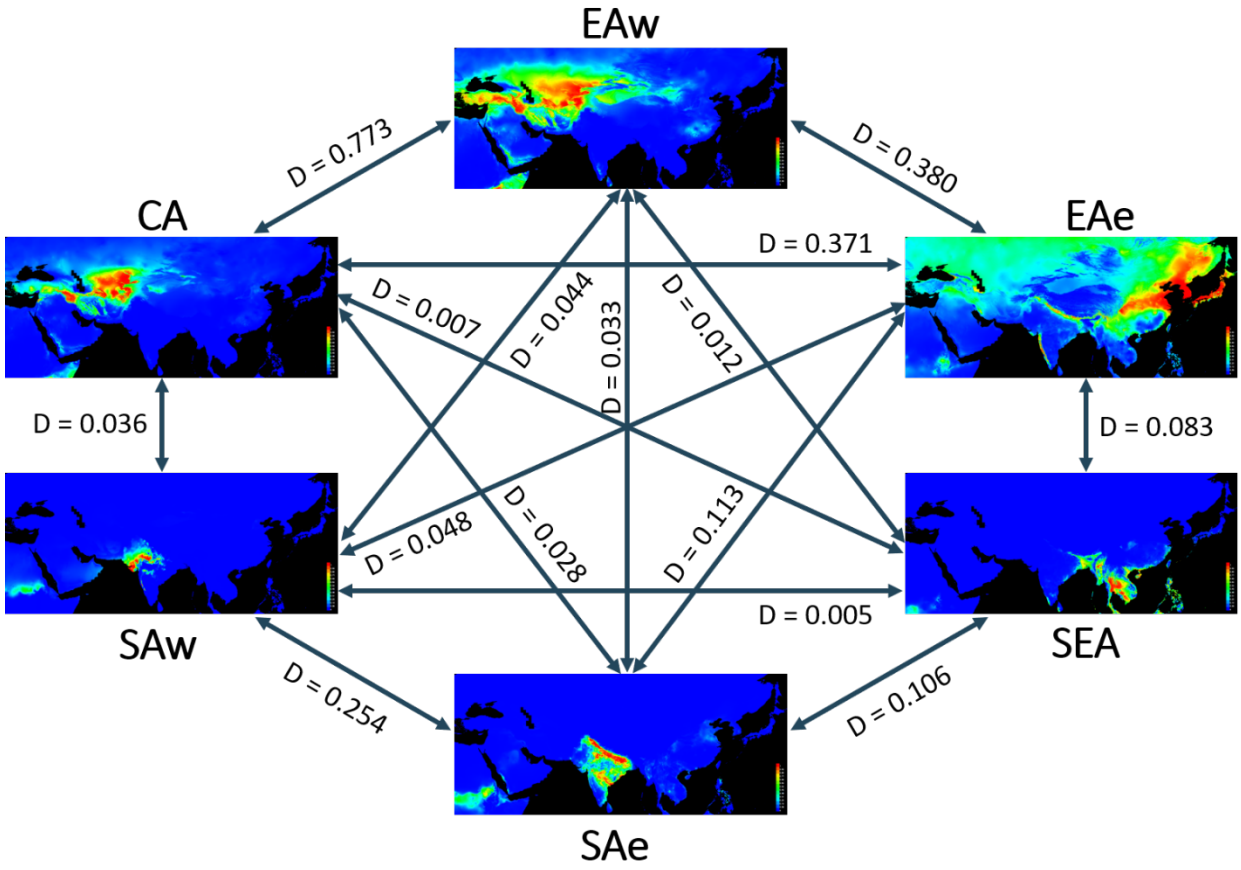

Figure 3-figure supplement 3. Predicted distributions of six groups based on monthly temperature and precipitation (May, July and September) during the summer growing season. Red colour indicates high suitability and blue indicates low suitability. Values between groups represent niche overlap measured using Schoener's D. Abbreviations: SAw: South Asia (west), SAe: South Asia (east); SEA: Southeast Asia; EAe: East Asia (east); EAw: East Asia (west) and CA: Central Asia.

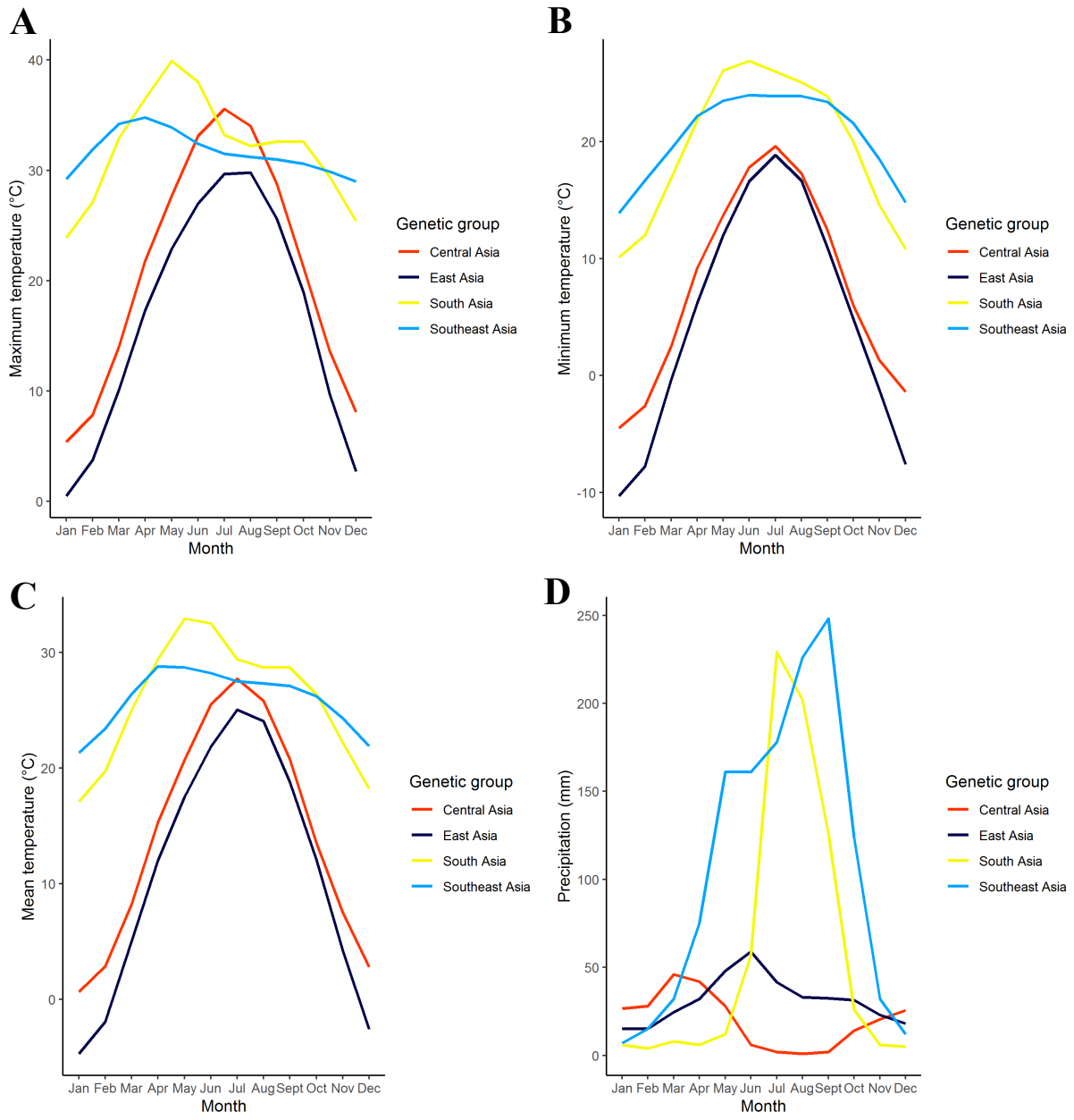

1030 **Figure 3-figure supplement 4.** Monthly temperature and precipitation variations among the four
1031 genetic groups. Monthly (A) maximum temperature, (B) minimum temperature, (C) mean
1032 temperature and (D) precipitation were computed based on median value among all accessions
1033 of a group. Genetic group were coloured the same as in Figure. 1.

1034

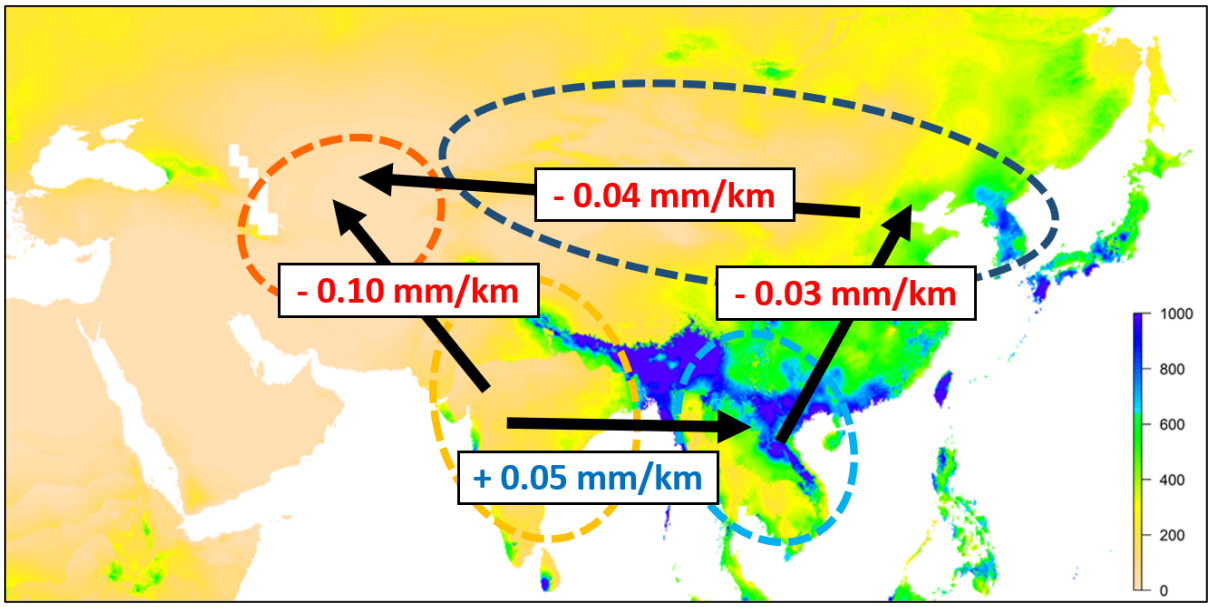

Figure 3-figure supplement 5. Environmental gradient across Asia. The value on each arrow indicates a change in mean precipitation for May, July and September (growth season) per kilometer. The background map is colored according to summer precipitation (Bio18, precipitation of warmest quarter, in mm).

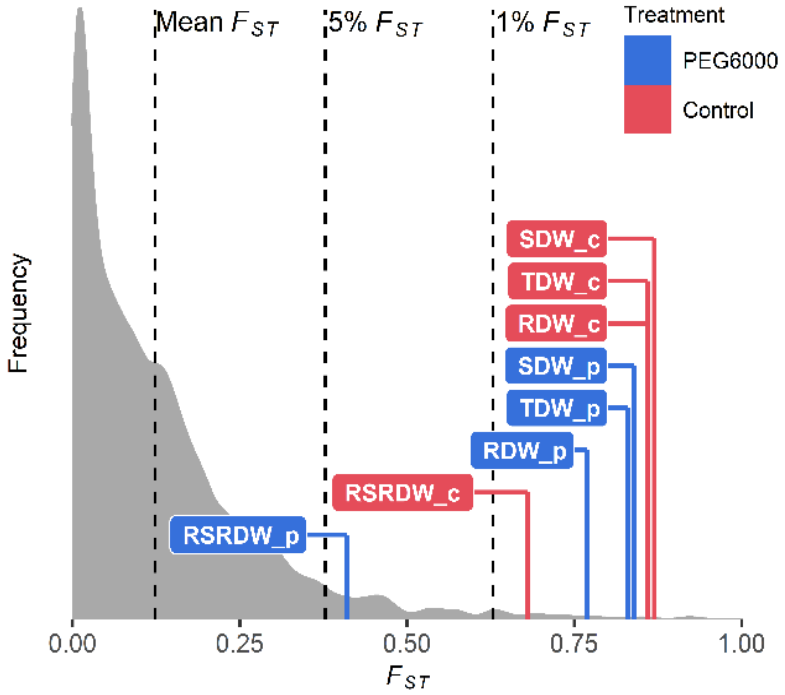

Figure 3-figure supplement 6. Comparison of Q_{ST}-F_{ST} for four drought-related traits under two environments. F_{ST} values (mean, 5% and 1%) were indicated by black dashed lines. The Q_{ST} for each trait was colored according to treatment and was calculated as Equation 1 in Materials and Methods. Abbreviations: RDW: root dry weight; SDW: shoot dry weight; TDW: total dry weight; RSRDW: root:shoot ratio dry weight; c: control; p: PEG6000.

1046 **Supplementary file 1.** Mungbean accessions from Vavilov Institute (VIR) collection
1047

Sample name	Country	Latitude	Longitude	NCBI SRA accession	NCBI Biosample accession
1.B	USA	NA	NA	SRR18125483	SAMN26179197
100.A	Cyprus	35.1856	33.3823	SRR18125482	SAMN26179198
101.A	Morocco	33.9716	-6.8498	SRR18125266	SAMN26179199
102.A	Israel	32.4971	35.4973	SRR18125200	SAMN26179200
103.A	Indonesia	-6.5971	106.806	SRR18125367	SAMN26179201
104.B	Russia	44.9003	131.8351	SRR18125356	SAMN26179202
105.A	Chile	-36.8305	-73.1167	SRR18125345	SAMN26179203
106.A	India	22.5587	88.2911	SRR18125298	SAMN26179204
107.A	India	22.5726	88.3639	SRR18125287	SAMN26179205
108.A	India	25.9821	85.6486	SRR18125276	SAMN26179206
109.A	Italy	41.9028	12.4964	SRR18125481	SAMN26179207
10A	China	47.1216	128.7382	SRR18125398	SAMN26179208
110.B	Portugal	38.7223	-9.1393	SRR18125387	SAMN26179209
111.A	Portugal	38.7223	-9.1393	SRR18125376	SAMN26179210
112.A	Russia	45.0347	39.0978	SRR18125329	SAMN26179211
113.A	Tajikistan	40.2675	69.6453	SRR18125318	SAMN26179212
114.B	India	31.5204	74.3587	SRR18125307	SAMN26179213
115.B	India	31.5204	74.3587	SRR18125476	SAMN26179214
116.A	Russia	49.6152	127.9945	SRR18125465	SAMN26179215
116.B	Russia	49.6152	127.9945	SRR18125454	SAMN26179216
117.B	Russia	44.0281	131.3273	SRR18125264	SAMN26179217
118.A	Russia	44.0118	131.3835	SRR18125253	SAMN26179218
119.A	Russia	44.39	132.558	SRR18125242	SAMN26179219
11A	China	47.1216	128.7382	SRR18125231	SAMN26179220
120.A	Argentina	-32.8895	-68.8458	SRR18125434	SAMN26179221
122.A	Japan	31.5969	130.5571	SRR18125423	SAMN26179222
123.B	Kyrgyzstan	55.4649	65.3054	SRR18125412	SAMN26179223
124.B	Ethiopia	12.9545	36.1573	SRR18125223	SAMN26179224
125.A	China	42.5246	87.5396	SRR18125212	SAMN26179225
126.A	China	42.5246	87.5396	SRR18125201	SAMN26179226
127.A	China	42.5246	87.5396	SRR18125199	SAMN26179227
128.A	Democratic Republic of the Congo	1.9293	30.0492	SRR18125198	SAMN26179228
128.B	Democratic Republic of the Congo	1.9293	30.0492	SRR18125197	SAMN26179229
129.A	Korea	37.5665	126.978	SRR18125196	SAMN26179230
12A	China	47.1216	128.7382	SRR18125195	SAMN26179231

13.A	Iran	32.4279	53.688	SRR18125194	SAMN26179232
130.A	Korea	37.5665	126.978	SRR18125371	SAMN26179233
131.A	Korea	37.5665	126.978	SRR18125370	SAMN26179234
132.B	Korea	40.3399	127.5101	SRR18125369	SAMN26179235
133.A	Korea	40.3399	127.5101	SRR18125368	SAMN26179236
134.A	Korea	40.3399	127.5101	SRR18125366	SAMN26179237
135.A	Korea	40.3399	127.5101	SRR18125365	SAMN26179238
136.A	Korea	40.3399	127.5101	SRR18125364	SAMN26179239
137.A	China	42.5246	87.5396	SRR18125363	SAMN26179240
138.A	China	39.4677	75.9938	SRR18125362	SAMN26179241
139.A	Uzbekistan	41.2995	69.2401	SRR18125361	SAMN26179242
14.B	Uzbekistan	39.7681	64.4556	SRR18125360	SAMN26179243
140.B	China	42.5246	87.5396	SRR18125359	SAMN26179244
141.A	China	43.8256	87.6168	SRR18125358	SAMN26179245
142.B	China	42.5246	87.5396	SRR18125357	SAMN26179246
144.A	Ukraine	48.4647	35.0462	SRR18125355	SAMN26179247
145.A	Brazil	-22.9329	-47.0738	SRR18125354	SAMN26179248
146.B	Kazakhstan	43.222	76.8512	SRR18125353	SAMN26179249
147.A	Turkey	39.7646	30.4559	SRR18125352	SAMN26179250
148.B	Turkey	39.7646	30.4559	SRR18125351	SAMN26179251
149.A	Ukraine	48.0386	30.9497	SRR18125350	SAMN26179252
151.A	Tajikistan	38.5598	68.787	SRR18125349	SAMN26179253
154.A	Brazil	-14.235	-51.9253	SRR18125348	SAMN26179254
155.A	United Kingdom	52.3555	-1.1743	SRR18125347	SAMN26179255
156.A	India	25.9821	85.6486	SRR18125346	SAMN26179256
157.A	India	25.9821	85.6486	SRR18125344	SAMN26179257
158.A	India	25.9821	85.6486	SRR18125343	SAMN26179258
159.B	India	25.9821	85.6486	SRR18125342	SAMN26179259
16.A	Uzbekistan	39.7681	64.4556	SRR18125341	SAMN26179260
160.A	Uzbekistan	40.8154	72.2837	SRR18125340	SAMN26179261
161.A	Uzbekistan	40.8154	72.2837	SRR18125339	SAMN26179262
162.A	South Africa	-26.7145	27.097	SRR18125338	SAMN26179263
163.A	South Africa	-26.7145	27.097	SRR18125337	SAMN26179264
164.A	South Africa	-26.7145	27.097	SRR18125336	SAMN26179265
165.B	USA	39.9526	-75.1652	SRR18125299	SAMN26179266
166.A	USA	39.9526	-75.1652	SRR18125297	SAMN26179267
167.B	Kyrgyzstan	42.8224	75.3179	SRR18125296	SAMN26179268
168.A	Kyrgyzstan	42.8224	75.3179	SRR18125295	SAMN26179269
17.B	Uzbekistan	39.7681	64.4556	SRR18125294	SAMN26179270
170.A	Russia	43.2562	46.5893	SRR18125293	SAMN26179271
171.A	Russia	43.2562	46.5893	SRR18125292	SAMN26179272

172.B	Iran	32.4279	53.688	SRR18125291	SAMN26179273
173.A	Iran	32.4279	53.688	SRR18125290	SAMN26179274
174.A	Korea	40.3399	127.5101	SRR18125289	SAMN26179275
175.A	Uzbekistan	40.2504	63.2032	SRR18125288	SAMN26179276
175.B	Uzbekistan	40.2504	63.2032	SRR18125286	SAMN26179277
176.A	Uzbekistan	40.2504	63.2032	SRR18125285	SAMN26179278
177.A	Uzbekistan	40.2504	63.2032	SRR18125284	SAMN26179279
178.A	Uzbekistan	40.2504	63.2032	SRR18125283	SAMN26179280
179.A	Uzbekistan	39.9208	66.4271	SRR18125282	SAMN26179281
18.B	Uzbekistan	39.7681	64.4556	SRR18125281	SAMN26179282
180.A	Uzbekistan	39.9208	66.4271	SRR18125280	SAMN26179283
181.A	Uzbekistan	39.9208	66.4271	SRR18125279	SAMN26179284
182.B	Uzbekistan	39.9208	66.4271	SRR18125278	SAMN26179285
183.A	Uzbekistan	40.3734	71.7978	SRR18125277	SAMN26179286
184.A	China	41.482754	85.626702	SRR18125275	SAMN26179287
187.A	China	38.10222	76.993816	SRR18125274	SAMN26179288
188.B	China	41.1675	80.2634	SRR18125273	SAMN26179289
189.A	China	41.1675	80.2634	SRR18125272	SAMN26179290
19.B	Iran	32.4279	53.688	SRR18125271	SAMN26179291
190.A	China	42.9513	89.1898	SRR18125270	SAMN26179292
191.A	China	41.175324	85.660861	SRR18125269	SAMN26179293
192.A	India	31.8183	75.2071	SRR18125268	SAMN26179294
193.A	India	31.326	75.5762	SRR18125267	SAMN26179295
193.B	India	31.326	75.5762	SRR18125265	SAMN26179296
194.A	India	30.3752	76.7821	SRR18125480	SAMN26179297
195.A	India	28.7041	77.1025	SRR18125407	SAMN26179298
195.B	India	28.7041	77.1025	SRR18125406	SAMN26179299
197.A	India	17.6599	75.9064	SRR18125405	SAMN26179300
199.A	Senegal	14.4974	-14.4524	SRR18125404	SAMN26179301
1A	USA	NA	NA	SRR18125403	SAMN26179302
201.B	Pakistan	31.5204	74.3587	SRR18125402	SAMN26179303
202.B	Canada	43.6502	-79.9036	SRR18125401	SAMN26179304
203.A	Ethiopia	9.3126	42.1227	SRR18125400	SAMN26179305
204.B	Indonesia	-6.5971	106.806	SRR18125399	SAMN26179306
205.A	Indonesia	-6.5971	106.806	SRR18125397	SAMN26179307
205.B	Indonesia	-6.5971	106.806	SRR18125396	SAMN26179308
206.A	Hungary	47.1625	19.5033	SRR18125395	SAMN26179309
207.A	Viet Nam	14.0583	108.2772	SRR18125394	SAMN26179310
21.B	Kazakhstan	51.1605	71.4704	SRR18125393	SAMN26179311
210.A	Afghanistan	36.6926	67.118	SRR18125392	SAMN26179312
212.A	Viet Nam	21.0278	105.8342	SRR18125391	SAMN26179313

215.A	Guinea	8.5383	-9.4728	SRR18125390	SAMN26179314
216.A	Uzbekistan	39.972132	65.558096	SRR18125389	SAMN26179315
217.B	Uzbekistan	40.162885	66.227209	SRR18125388	SAMN26179316
218.A	Uzbekistan	40.013465	64.943243	SRR18125386	SAMN26179317
219.A	Turkmenistan	40.243331	59.540314	SRR18125385	SAMN26179318
22.B	Kazakhstan	42.3417	69.5901	SRR18125384	SAMN26179319
220.A	Turkmenistan	40.243331	59.540314	SRR18125383	SAMN26179320
223.A	Uzbekistan	40.483568	70.546311	SRR18125382	SAMN26179321
224.A	Iran	32.6539	51.666	SRR18125381	SAMN26179322
225.A	Pakistan	30.3753	69.3451	SRR18125380	SAMN26179323
226.B	Pakistan	30.3753	69.3451	SRR18125379	SAMN26179324
227.A	Pakistan	30.3753	69.3451	SRR18125378	SAMN26179325
228.B	Turkmenistan	39.0041	63.5688	SRR18125377	SAMN26179326
229.A	Pakistan	31.4504	73.135	SRR18125375	SAMN26179327
23.A	Kazakhstan	42.3417	69.5901	SRR18125374	SAMN26179328
230.A	Pakistan	31.4504	73.135	SRR18125373	SAMN26179329
230.B	Pakistan	31.4504	73.135	SRR18125372	SAMN26179330
231.A	Tanzania	-6.369	34.8888	SRR18125335	SAMN26179331
232.A	Iran	34.3277	47.0778	SRR18125334	SAMN26179332
233.A	Iran	32.4279	53.688	SRR18125333	SAMN26179333
234.A	India	28.6139	77.209	SRR18125332	SAMN26179334
235.A	Pakistan	33.5651	73.0169	SRR18125331	SAMN26179335
235.B	Pakistan	33.5651	73.0169	SRR18125330	SAMN26179336
236.A	Pakistan	34.0155	71.6888	SRR18125328	SAMN26179337
237.A	Pakistan	28.6001	77.227	SRR18125327	SAMN26179338
238.A	Egypt	26.8206	30.8025	SRR18125326	SAMN26179339
239.A	Kazakhstan	44.7689	77.5573	SRR18125325	SAMN26179340
24.A	Uzbekistan	41.4065	60.3685	SRR18125324	SAMN26179341
240.A	Uzbekistan	39.4065	67.1418	SRR18125323	SAMN26179342
240.B	Uzbekistan	39.4065	67.1418	SRR18125322	SAMN26179343
241.A	Uzbekistan	40.023044	67.433724	SRR18125321	SAMN26179344
242.A	Uzbekistan	39.982851	67.486778	SRR18125320	SAMN26179345
244.A	Uzbekistan	41.773406	63.780613	SRR18125319	SAMN26179346
245.A	Kazakhstan	43.47491	75.335144	SRR18125317	SAMN26179347
246.A	Algeria	35.6971	-0.6308	SRR18125316	SAMN26179348
247.A	Tanzania	-5.0425	32.8197	SRR18125315	SAMN26179349
249.A	Australia	-32.9283	151.7817	SRR18125314	SAMN26179350
25.A	Uzbekistan	41.4065	60.3685	SRR18125313	SAMN26179351
250.B	Russia	NA	NA	SRR18125312	SAMN26179352
251.B	USA	NA	NA	SRR18125311	SAMN26179353
252.A	Afghanistan	34.7602	69.8121	SRR18125310	SAMN26179354

253.A	Afghanistan	34.7602	69.8121	SRR18125309	SAMN26179355
254.A	Yemen	15.5527	48.5164	SRR18125308	SAMN26179356
254.B	Yemen	15.5527	48.5164	SRR18125306	SAMN26179357
255.A	Afghanistan	36.6926	67.118	SRR18125305	SAMN26179358
256.A	Afghanistan	36.6926	67.118	SRR18125304	SAMN26179359
257.B	Afghanistan	36.6926	67.118	SRR18125303	SAMN26179360
258.B	Afghanistan	33.9391	67.71	SRR18125302	SAMN26179361
259.B	Colombia	4.5709	-74.2973	SRR18125301	SAMN26179362
26.B	Uzbekistan	41.4065	60.3685	SRR18125300	SAMN26179363
260.A	Philippines	14.5995	120.9842	SRR18125479	SAMN26179364
261.B	Kenya	-1.2921	36.8219	SRR18125478	SAMN26179365
262.A	Kenya	-1.2921	36.8219	SRR18125477	SAMN26179366
263.A	Kenya	-1.2921	36.8219	SRR18125475	SAMN26179367
264.A	Kenya	-1.2921	36.8219	SRR18125474	SAMN26179368
265.B	Kenya	-1.2921	36.8219	SRR18125473	SAMN26179369
266.A	Kenya	-1.2921	36.8219	SRR18125472	SAMN26179370
267.A	Kenya	-1.2921	36.8219	SRR18125471	SAMN26179371
268.A	Kenya	-1.2921	36.8219	SRR18125470	SAMN26179372
269.B	Kenya	-1.2921	36.8219	SRR18125469	SAMN26179373
27.A	Uzbekistan	39.7681	64.4556	SRR18125468	SAMN26179374
270.A	Kenya	-1.2921	36.8219	SRR18125467	SAMN26179375
271.A	South Korea	35.8987	127.0392	SRR18125466	SAMN26179376
272.A	Australia	NA	NA	SRR18125464	SAMN26179377
273.A	Kenya	-1.2921	36.8219	SRR18125463	SAMN26179378
274.A	Kenya	-1.2921	36.8219	SRR18125462	SAMN26179379
275.A	Kenya	-1.2921	36.8219	SRR18125461	SAMN26179380
276.A	Kenya	-1.2921	36.8219	SRR18125460	SAMN26179381
277.B	Kazakhstan	43.1521	68.2581	SRR18125459	SAMN26179382
278.B	Kazakhstan	43.0631	69.0851	SRR18125458	SAMN26179383
279.A	Kazakhstan	41.5295	69.4133	SRR18125457	SAMN26179384
28.A	Russia	42.1432	47.095	SRR18125456	SAMN26179385
280.B	Kazakhstan	41.5295	69.4133	SRR18125455	SAMN26179386
281.B	South Korea	35.8987	127.0392	SRR18125453	SAMN26179387
282.B	South Korea	35.8987	127.0392	SRR18125452	SAMN26179388
283.B	South Korea	35.8987	127.0392	SRR18125451	SAMN26179389
284.A	Tajikistan	38.0116	71.003	SRR18125450	SAMN26179390
285.A	Tajikistan	37.074793	67.957222	SRR18125449	SAMN26179391
286.A	Tajikistan	37.028926	68.004059	SRR18125448	SAMN26179392
287.A	Tajikistan	39.179338	68.012339	SRR18125447	SAMN26179393
288.A	Philippines	14.5995	120.9842	SRR18125446	SAMN26179394
289.B	Philippines	14.5995	120.9842	SRR18125445	SAMN26179395

290.A	China	40.2374	116.2305	SRR18125444	SAMN26179396
290.B	China	40.2374	116.2305	SRR18125263	SAMN26179397
291.A	China	40.2374	116.2305	SRR18125262	SAMN26179398
292.A	China	30.7378	112.2384	SRR18125261	SAMN26179399
293.A	China	30.7378	112.2384	SRR18125260	SAMN26179400
294.A	China	40.2374	116.2305	SRR18125259	SAMN26179401
295.B	China	37.8957	114.9042	SRR18125258	SAMN26179402
296.A	China	37.8957	114.9042	SRR18125257	SAMN26179403
297.A	China	47.1216	128.7382	SRR18125256	SAMN26179404
298.B	China	47.1216	128.7382	SRR18125255	SAMN26179405
299.A	China	40.2374	116.2305	SRR18125254	SAMN26179406
2A	China	47.1216	128.7382	SRR18125252	SAMN26179407
3.B	China	47.1216	128.7382	SRR18125251	SAMN26179408
30.A	Russia	42.1432	47.095	SRR18125250	SAMN26179409
300.A	China	47.1216	128.7382	SRR18125249	SAMN26179410
31.A	Russia	42.1432	47.095	SRR18125248	SAMN26179411
32.B	Russia	42.1432	47.095	SRR18125247	SAMN26179412
33.A	USA	NA	NA	SRR18125246	SAMN26179413
34.A	USA	NA	NA	SRR18125245	SAMN26179414
34.B	USA	NA	NA	SRR18125244	SAMN26179415
35.A	Russia	NA	NA	SRR18125243	SAMN26179416
36.A	Russia	43.1198	131.8869	SRR18125241	SAMN26179417
37.A	USA	NA	NA	SRR18125240	SAMN26179418
38.B	China	44.9188	130.5244	SRR18125239	SAMN26179419
39.A	Iran	36.3394	59.4698	SRR18125238	SAMN26179420
3A	China	47.1216	128.7382	SRR18125237	SAMN26179421
40.B	Iran	36.3394	59.4698	SRR18125236	SAMN26179422
41.B	Iran	32.4279	53.688	SRR18125235	SAMN26179423
42.A	Iran	32.4279	53.688	SRR18125234	SAMN26179424
43.A	Iran	32.4279	53.688	SRR18125233	SAMN26179425
44.B	Turkmenistan	37.9153	58.0897	SRR18125232	SAMN26179426
45.A	Turkmenistan	37.9153	58.0897	SRR18125230	SAMN26179427
46.A	Turkmenistan	37.9153	58.0897	SRR18125443	SAMN26179428
47.A	Turkmenistan	37.9153	58.0897	SRR18125442	SAMN26179429
48.B	Turkmenistan	37.9153	58.0897	SRR18125441	SAMN26179430
49.B	Turkmenistan	37.9172	58.0907	SRR18125440	SAMN26179431
4A	China	47.1216	128.7382	SRR18125439	SAMN26179432
5.B	China	47.1216	128.7382	SRR18125438	SAMN26179433
50.A	Turkmenistan	37.9172	58.0907	SRR18125437	SAMN26179434
51.B	Turkmenistan	37.9601	58.3261	SRR18125436	SAMN26179435
52.A	Turkmenistan	37.9601	58.3261	SRR18125435	SAMN26179436

53.B	USA	40.1605	-103.2144	SRR18125433	SAMN26179437
54.A	USA	40.1605	-103.2144	SRR18125432	SAMN26179438
55.B	Ukraine	48.3794	31.1656	SRR18125431	SAMN26179439
56.A	Kazakhstan	43.3667	68.4094	SRR18125430	SAMN26179440
57.A	Iran	34.7608	48.3988	SRR18125429	SAMN26179441
58.A	Iran	35.6892	51.389	SRR18125428	SAMN26179442
59.B	Kazakhstan	43.3667	68.4094	SRR18125427	SAMN26179443
6.B	China	47.1216	128.7382	SRR18125426	SAMN26179444
60.A	Kazakhstan	42.2663	68.1431	SRR18125425	SAMN26179445
61.A	Uzbekistan	41.2995	69.2401	SRR18125424	SAMN26179446
62.A	Uzbekistan	41.2995	69.2401	SRR18125422	SAMN26179447
63.A	Uzbekistan	41.2995	69.2401	SRR18125421	SAMN26179448
64.B	Uzbekistan	41.2995	69.2401	SRR18125420	SAMN26179449
65.B	Uzbekistan	41.2995	69.2401	SRR18125419	SAMN26179450
66.B	Uzbekistan	41.2995	69.2401	SRR18125418	SAMN26179451
67.A	Uzbekistan	41.2995	69.2401	SRR18125417	SAMN26179452
68.A	Uzbekistan	41.2995	69.2401	SRR18125416	SAMN26179453
69.A	Uzbekistan	40.4915	68.7811	SRR18125415	SAMN26179454
70.A	Uzbekistan	39.627	66.975	SRR18125414	SAMN26179455
71.A	Uzbekistan	39.627	66.975	SRR18125413	SAMN26179456
72.A	Uzbekistan	39.627	66.975	SRR18125411	SAMN26179457
73.B	Uzbekistan	39.627	66.975	SRR18125410	SAMN26179458
74.A	Uzbekistan	39.627	66.975	SRR18125409	SAMN26179459
75.A	Uzbekistan	39.627	66.975	SRR18125408	SAMN26179460
76.A	Uzbekistan	41.2995	69.2401	SRR18125229	SAMN26179461
77.A	Uzbekistan	39.7681	64.4556	SRR18125228	SAMN26179462
79.B	Uzbekistan	39.7681	64.4556	SRR18125227	SAMN26179463
7A	China	47.1216	128.7382	SRR18125226	SAMN26179464
8.B	China	47.1216	128.7382	SRR18125225	SAMN26179465
81.B	Afghanistan	34.1769	61.7006	SRR18125224	SAMN26179466
82.B	Afghanistan	34.1769	61.7006	SRR18125222	SAMN26179467
83.A	Afghanistan	34.1769	61.7006	SRR18125221	SAMN26179468
84.A	Afghanistan	34.1769	61.7006	SRR18125220	SAMN26179469
85.A	Afghanistan	34.1769	61.7006	SRR18125219	SAMN26179470
86.A	Afghanistan	36.6153	66.9293	SRR18125218	SAMN26179471
88.B	Afghanistan	NA	NA	SRR18125217	SAMN26179472
89.B	Afghanistan	33.9391	67.71	SRR18125216	SAMN26179473
90.B	Uzbekistan	NA	NA	SRR18125215	SAMN26179474
91.A	Japan	35.719	139.7456	SRR18125214	SAMN26179475
92.A	Japan	35.719	139.7456	SRR18125213	SAMN26179476
93.B	Armenia	40.0691	45.0382	SRR18125211	SAMN26179477

94.A	Iran	35.102	59.1042	SRR18125210	SAMN26179478
95.A	Azerbaijan	40.4093	49.8671	SRR18125209	SAMN26179479
96.A	Azerbaijan	40.1431	47.5769	SRR18125208	SAMN26179480
97.A	Turkmenistan	39.0041	63.5688	SRR18125207	SAMN26179481
98.B	Panama	9.3593	-79.8999	SRR18125206	SAMN26179482
99.A	Panama	9.3593	-79.8999	SRR18125205	SAMN26179483
99.B	Panama	9.3593	-79.8999	SRR18125204	SAMN26179484
9A	China	47.1216	128.7382	SRR18125203	SAMN26179485
M7.A	India	31.5204	74.3587	SRR18125202	SAMN26179486

1048

Supplementary file 2. Outgroup *f*3 statistics among all possible combinations of genetic group pairs

Outgroup (C)	Source 1 (A)	Source2 (B)	*f*3	Standard error	Z-score	Significant
sublobata	CA	EA	0.232	0.005	42.66	Yes
sublobata	CA	SA	0.209	0.005	38.41	Yes
sublobata	CA	SEA	0.213	0.005	39.03	Yes
sublobata	EA	SA	0.209	0.005	38.79	Yes
sublobata	EA	SEA	0.218	0.005	40.75	Yes
sublobata	SA	SEA	0.211	0.005	39.41	Yes

Abbreviations: SA, South Asia; SEA, Southeast Asia; EA, East Asia and CA, Central Asia (*f*3 statistics with Z-score > |3| are considered significant)

Supplementary file 3. Admixture *f*3 statistics among all possible population trios

Target (C)	Source1 (A)	Source2 (B)	*f*3	Standard error	Z-score	Significant
EA	SA	CA	0.005	0.001	4.82	Yes
EA	SEA	CA	-0.001	0.001	-0.51	No
EA	SEA	SA	0.020	0.002	13.48	Yes
SEA	CA	EA	0.030	0.002	14.7	Yes
SEA	SA	CA	0.014	0.002	8.82	Yes
SEA	SA	EA	0.009	0.001	6.86	Yes
SA	CA	EA	0.032	0.002	16.66	Yes
SA	CA	SEA	0.011	0.001	9.02	Yes
SA	EA	SEA	0.017	0.001	12.91	Yes
CA	EA	SA	0.011	0.001	9.55	Yes
CA	EA	SEA	0.016	0.002	10.37	Yes
CA	SEA	SA	0.031	0.002	15.65	Yes

Abbreviations: SA, South Asia; SEA, Southeast Asia; EA, East Asia and CA, Central Asia (*f*3 statistics with Z-score > |3| are considered significant, but only negative *f3* statistics denote the target population being admixed from source1 and source2.)

Supplementary file 4. Mantel tests for isolation by distance of inferred genetic group ($Q \geq 0.5$)

Group	***r***	***P***
SA	0.4319	0.008*
SEA	0.3312	0.041*
EA	0.0461	0.052
CA	0.0070	0.435
Southern	0.2934	0.001*
Northern	0.2777	0.001*

Abbreviations: SA, South Asia; SEA, Southeast Asia; EA, East Asia; CA, Central Asia; *r*, Mantel correlation; significance level * $P < 0.05$

Supplementary file 5. Description of bioclimatic variables used in ecological niche modelling

Bioclimatic variable	Variable	Unit
Bio1	Annual mean temperature	ºC
Bio2	Mean diurnal range (mean of monthly (max temp - min temp))	ºC
Bio3	Isothermality (Bio2/Bio7) (×100)	ºC
Bio4	Temperature seasonality (standard deviation ×100)	ºC
Bio5	Max temperature of warmest month	ºC
Bio6	Min temperature of coldest month	ºC
Bio7	Temperature annual range (Bio5-Bio6)	ºC
Bio8	Mean temperature of wettest quarter	ºC
Bio9	Mean temperature of driest quarter	ºC
Bio10	Mean temperature of warmest quarter	ºC
Bio11	Mean temperature of coldest quarter	ºC
Bio12	Annual precipitation	mm
Bio13	Precipitation of wettest month	mm
Bio14	Precipitation of driest month	mm
Bio15	Precipitation seasonality (coefficient of variation)	mm
Bio16	Precipitation of wettest quarter	mm
Bio17	Precipitation of driest quarter	mm
Bio18	Precipitation of warmest quarter	mm
Bio19	Precipitation of coldest quarter	mm

Supplementary file 6. Pearson's correlation coefficient between pairs of bioclimatic variables (denoted in lower triangle)

Bioclimatic variable	Bio1	Bio2	Bio3	Bio4	Bio5	Bio6	Bio7	Bio8	Bio9	Bio10	Bio11	Bio12	Bio13	Bio14	Bio15	Bio16	Bio17	Bio18	Bio19
Bio1	1	-	-	-	-	-	-	-	-	-	-	-	-	-	-	-	-	-	-
Bio2	0.087	1	-	-	-	-	-	-	-	-	-	-	-	-	-	-	-	-	-
Bio3	0.732	0.321	1	-	-	-	-	-	-	-	-	-	-	-	-	-	-	-	-
Bio4	-0.814	0.011	-0.876	1	-	-	-	-	-	-	-	-	-	-	-	-	-	-	-
Bio5	0.872	0.258	0.455	-0.449	1	-	-	-	-	-	-	-	-	-	-	-	-	-	-
Bio6	0.971	-0.038	0.779	-0.911	0.749	1	-	-	-	-	-	-	-	-	-	-	-	-	-
Bio7	-0.773	0.225	-0.784	0.973	-0.377	-0.896	1	-	-	-	-	-	-	-	-	-	-	-	-
Bio8	0.595	-0.066	0.383	-0.398	0.522	0.530	-0.392	1	-	-	-	-	-	-	-	-	-	-	-
Bio9	0.901	0.122	0.663	-0.759	0.803	0.896	-0.715	0.257	1	-	-	-	-	-	-	-	-	-	-
Bio10	0.915	0.129	0.472	-0.513	0.983	0.808	-0.472	0.590	0.815	1	-	-	-	-	-	-	-	-	-
Bio11	0.977	0.050	0.814	-0.918	0.760	0.994	-0.881	0.544	0.894	0.811	1	-	-	-	-	-	-	-	-
Bio12	0.237	-0.513	0.244	-0.397	-0.030	0.327	-0.477	0.293	0.121	0.073	0.303	1	-	-	-	-	-	-	-
Bio13	0.276	-0.341	0.289	-0.403	0.040	0.332	-0.438	0.342	0.142	0.124	0.330	0.926	1	-	-	-	-	-	-
Bio14	-0.084	-0.620	-0.151	-0.011	-0.205	0.013	-0.154	0.039	-0.120	-0.126	-0.048	0.494	0.233	1	-	-	-	-	-
Bio15	0.258	0.528	0.405	-0.263	0.208	0.191	-0.128	0.302	0.156	0.189	0.262	-0.024	0.213	-0.521	1	-	-	-	-
Bio16	0.271	-0.364	0.283	-0.406	0.028	0.333	-0.446	0.330	0.141	0.115	0.328	0.950	0.992	0.258	0.178	1	-	-	-
Bio17	-0.050	-0.639	-0.110	-0.058	-0.194	0.052	-0.203	0.062	-0.089	-0.110	-0.009	0.555	0.294	0.988	-0.508	0.321	1	-	-
Bio18	-0.031	-0.453	-0.011	-0.119	-0.257	0.027	-0.210	0.245	-0.184	-0.144	0.015	0.805	0.741	0.392	0.016	0.766	0.438	1	-
Bio19	0.177	-0.270	0.266	-0.279	0.048	0.263	-0.335	-0.010	0.218	0.080	0.227	0.460	0.353	0.468	-0.196	0.356	0.490	0.115	1

Supplementary file 7. Comparison of bioclimatic variables among the four genetic groups analysed with multivariate analysis of variance (MANOVA)

Predictor	Test statistic	Df	Observed value	F value	Num. Df	Den. Df	*P*
Genetic group	Pillai	3	1.790	44.215	24	717	< 2e-16
	Wilks	3	0.024	74.690	24	688	< 2e-16
	Hotelling-Lawley	3	12.716	124.870	24	707	< 2e-16
	Roy	3	10.777	321.960	8	239	< 2e-16

Df = degree of freedom among groups; Num. Df = degrees of freedom of the model; Den. Df = degree of freedom of residual

Supplementary file 8. Summary of analysis of variance (ANOVA) for bioclimatic variables

Bioclimatic variable	Df	Sum square	Mean square	F value	*P*
Bio1 (Annual temperature)	3	183.688	61.229	235.97	<2.2e-16
Bio2 (Mean diurnal temperature range)	3	66.253	22.085	29.813	<2.2e-16
Bio3 (Isothermality)	3	188.031	62.677	259.34	<2.2e-16
Bio8 (Mean temperature of wettest quarter)	3	177.063	59.021	205.91	<2.2e-16
Bio12 (Annual precipitation)	3	157.890	52.630	144.11	<2.2e-16
Bio14 (Precipitation of driest month)	3	29.859	9.952	11.183	<6.6e-07
Bio15 (Precipitation seasonality)	3	119.810	39.938	76.62	<2.2e-16
Bio19 (Precipitation of coldest quarter)	3	44.212	14.737	17.732	< 1.9e-10

Df = degree of freedom

Supplementary file 9. Correlation between eight bioclimatic variables and climatic PC axes 1 to 4

Bioclimatic variable	PC1	PC2	PC3	PC4
Bio1 (Annual temperature)	**-0.445**	-0.107	0.390	-0.056
Bio2 (Mean diurnal temperature range)	0.193	**-0.564**	0.062	0.253
Bio3 (Isothermality)	**-0.430**	-0.082	**0.492**	-0.184
Bio8 (Mean temperature of wettest quarter)	**-0.486**	0.042	-0.287	0.049
Bio12 (Annual precipitation)	**-0.401**	0.366	0.066	0.202
Bio14 (Precipitation of driest month)	0.017	**0.582**	-0.248	0.259
Bio15 (Precipitation seasonality)	-0.323	-0.365	-0.292	**0.667**
Bio19 (Precipitation of coldest quarter)	0.279	0.235	**0.607**	**0.587**

(Correlation coefficients with absolute values higher than 0.4 are in bold.)

Supplementary file 10. Comparison of summer growing season data including temperature and precipitation of May, July and September among the four genetic groups analysed with multivariate analysis of variance (MANOVA)

Predictor	Test statistic	Df	Observed value	F value	Num. Df	Den. Df	*P*
Genetic group	Pillai	3	1.915	70.907	18	723	< 2e-16
	Wilks	3	0.010	156.350	18	676	< 2e-16
	Hotelling-Lawley	3	19.873	262.400	18	713	< 2e-16
	Roy	3	15.400	618.570	6	241	< 2e-16

Df = degree of freedom among groups; Num. Df = degrees of freedom of the model; Den. Df = degree of freedom of residual

Supplementary file 11. ANOVA table for all evaluated field traits (phenology, reproduction and size) as well as drought-related traits

Trait	Garden	Model r^2	Group *F*	Group *P*	SEA[1]	SA[1]	CA[1]	Tukey[2]
Phenology:								
Days to 50% flowering	Pakistan 2015	0.2388	7.2144	0.0019*	-0.3702	0.6296	-0.3525	B,A,B
Days to 50% flowering	Taiwan 1984	0.5266	25.5887	<.0001*	0.5723	0.3197	-1.0685	A,A,B
Days to 50% flowering	Taiwan 2018	0.4465	18.5544	<.0001*	0.0974	0.6569	-0.9633	A,A,B
Reproduction:								
100 seed weight, g	Pakistan 2015	0.4722	20.5761	<.0001*	0.9050	-0.6397	-0.2756	A,B,B
Pod length, cm	Pakistan 2015	0.2621	8.1698	0.0009*	0.6810	-0.2605	-0.4896	A,B,B
Pod length, cm	Taiwan 1984	0.7173	58.3615	<.0001*	1.0524	-0.1980	-1.0232	A,B,C
Pods per plant	Pakistan 2015	0.4471	18.5988	<.0001*	-0.6441	0.8455	-0.3062	B,A,B
1000 seed weight, g	Taiwan 1984	0.6248	38.3053	<.0001*	0.9979	-0.8380	-0.1340	A,C,B
Seed yield per plant, g	Pakistan 2015	0.4666	20.1225	<.0001*	-0.6210	0.8752	-0.3712	B,A,B
Seeds per pod	Pakistan 2015	0.1300	3.4372	0.0406*	-0.4875	0.2418	0.2806	A,A,A
Seeds per pod	Taiwan 1984	0.1611	4.4168	0.0176*	0.1413	0.3386	-0.6107	AB,A,B
Plant size:								
Petiole length, cm	Pakistan 2015	0.2943	9.5907	0.0003*	0.5435	0.0878	-0.7798	A,A,B
Plant height, cm	Pakistan 2015	0.0001	0.0024	0.9976	0.0075	0.0055	-0.0158	A,A,A
Plant height at flowering, cm	Taiwan 1984	0.3981	15.2115	<.0001*	0.4811	0.3024	-0.9705	A,A,B
Plant height at maturity, cm	Taiwan 1984	0.5472	27.8000	<.0001*	0.3480	0.5605	-1.1362	A,A,B
Primary leaf length, cm	Taiwan 1984	0.5454	27.5930	<.0001*	0.9813	-0.4212	-0.6253	A,B,B
Primary leaf width, cm	Taiwan 1984	0.6053	35.2773	<.0001*	1.0244	-0.6010	-0.4313	A,B,B
Terminal leaflet length, cm	Pakistan 2015	0.2186	6.4340	0.0034*	0.3062	0.2643	-0.7167	A,A,B
Terminal leaflet width, cm	Pakistan 2015	0.1680	4.6458	0.0145*	0.4361	0.0387	-0.5734	A,AB,B
Drought (PEG6000):								

Shoot dry weight (SDW), mg	NTU 2021	0.5998	36.7246	<.0001*	1.0508	-0.5607	-0.5483	A,B,B
Root dry weight (RDW), mg	NTU 2021	0.5964	36.2048	<.0001*	1.0299	-0.6933	-0.3336	A,B,B
Total dry weight (TDW), mg	NTU 2021	0.5934	35.7555	<.0001*	1.0448	-0.5883	-0.5028	A,B,B
Root:Shoot ratio dry weight (RSRDW)	NTU 2021	0.3261	11.8577	<.0001*	-0.2316	-0.4342	0.9112	B,B,A
Drought (Control):								
Shoot dry weight (SDW), mg	NTU 2021	0.5779	33.5453	<.0001*	1.0275	-0.4709	-0.6484	A,B,B
Root dry weight (RDW), mg	NTU 2021	0.5205	26.5962	<.0001*	0.9716	-0.6077	-0.3811	A,B,B
Total dry weight (TDW), mg	NTU 2021	0.5638	31.6722	<.0001*	1.0195	-0.5374	-0.5430	A,B,B
Root:Shoot ratio dry weight (RSRDW)	NTU 2021	0.1753	5.2083	0.0089*	-0.3036	-0.2004	0.6773	B,B,A

*Significant at $P < 0.05$; 1: least-square means of each group after inverse normal transformation of raw data; 2: levels not connected by same letter are significantly different.

Supplementary file 12. Mean of eight bioclimatic variables of the genetic groups

Bioclimatic variable	Northeast Asia (N = 37) Mean ± SD	Northwest Asia (N = 45) Mean ± SD	Southeast Asia (N = 45) Mean ± SD	South Asia (N = 49) Mean ± SD	Central Asia (N = 72) Mean ± SD
Bio1	62.49 ± 55.39	117.58 ± 54.30	256.47 ± 19.29	255.57 ± 14.80	128.72 ± 41.10
Bio2	115.22 ± 15.44	124.38 ± 20.14	102.02 ± 16.11	127.24 ± 16.12	130.08 ± 13.89
Bio3	25.14 ± 2.04	31.02 ± 4.47	51.58 ± 7.19	42.8 ± 4.58	32.4 ± 3.52
Bio8	207.86 ± 31.97	107.89 ± 67.90	271.47 ± 11.68	283.92 ± 23.02	92.04 ± 42.23
Bio12	821.59 ± 299.98	301.24 ± 201.00	1477.69 ± 380.18	750.39 ± 329.19	285.67 ± 145.24
Bio14	12.14 ± 11.72	5.18 ± 8.99	6.33 ± 4.34	2.47 ± 3.44	2.51 ± 4.98
Bio15	95.35 ± 24.52	65.4 ± 20.35	84.78 ± 7.25	124.47 ± 23.48	70.92 ± 12.92
Bio19	42.51 ± 38.23	88.33 ± 67.16	48.02 ± 24.91	34 ± 33.99	92.15 ± 45.19